Ecological Informatics 97 (2026) 103897

Contents lists available at ScienceDirect

Ecological Informatics

journal homepage: www.elsevier.com/locate/ecolinf

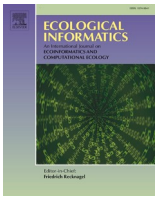

Tree-quest: A citizen science app for collecting single-tree information

Milutin Milenković [a,*], Florian Hofhansl [a], Rudi Weinacker [a], Tobias Sturn [a], Santosh Karanam [a], Benjamin Wild [b], Markus Hollaus [b], Christoph Neumayr [b], Anna Iglseder [b], Norbert Pfeifer [b], Luca Zappa [c], Viktor J. Bruckman [d], Roman Breitfuss-Schiffer [e], Benjamin Schumacher [f], Hugo Gresse [g], Alexis Joly [g], Pierre Bonnet [h], Dmitry Schepaschenko [a], Linda See [a], Ian McCallum [a], Steffen Fritz [a]

[a] International Institute for Applied Systems Analysis (IIASA), Laxenburg, Austria
[b] Technical University of Vienna (TUW), Vienna, Austria
[c] Austrian Environment Agency, Vienna, Austria
[d] The Austrian Academy of Sciences, Vienna, Austria
[e] Tree.lyFlexCo, Dornbirn, Austria
[f] Austrian Federal Office and Research Centre for Forests (BFW), Vienna, Austria
[g] National Institute for Research in Digital Science and Technology (INRIA), Laboratory of Computer Science, Robotics and Microelectronics of Montpellier (LIRMM), Montpellier, France
[h] AMAP Lab, University of Montpellier; French Agricultural Research Centre for International Development (CIRAD), French National Centre for Scientific Research (CNRS), National Research Institute for Agriculture, Food and Environment (INRAE), French National Research Institute for Sustainable Development (IRD), Montpellier, France

ARTICLE INFO

Keywords:
Citizen science
Crowdsourcing
In situ
Mobile phone
Remote sensing
Augmented reality
Aboveground biomass

ABSTRACT

Quantifying single-tree structural attributes through crowdsourcing has strong potential to expand the availability and timeliness of ground-based data for terrestrial carbon assessment of trees both within and outside forests. Recently, a number of freely available augmented-reality (AR) mobile apps have enabled accurate measurement of carbon-relevant single-tree attributes such as tree diameter and height. However, crowdsourcing with these apps is constrained by limited data quality control and the need for a separate species-identification app. Here, we present a crowdsourcing-ready workflow with our novel and freely available Tree-Quest (TQ) app that, in addition to AR-based measurements of tree height and diameter, integrates the Pl@ntNet API for species identification and includes a crowdsourced data quality curation step based on its AR images. We have compiled a dataset comprising 700 measurements of single trees acquired from 30 volunteers across two Austrian urban environments. The trees had diameters at breast height (DBHs) ranging from 11.9 cm to 161.2 cm and tree heights (THs) ranging from 4.6 m to 29.0 m. The dataset was evaluated for the accuracy of the identified tree attributes, including TH and DBH. Compared with professional forest inventory measurements, volunteers using TQ achieved a mean absolute error (MAE) of 3 cm for DBH ($R^2 = 0.97$; rMAE = 6%) and 1.5 m for TH ($R^2 = 0.91$; rMAE = 11%). TQ results were also consistent with DBH and TH measurements acquired with other freely available mobile applications. Besides these encouraging results, TQ can work offline and is highly modular, allowing the design of customized quests, targeted questionnaires, and uploads of the collected information to a central database to share single tree data openly, and supports user interaction through gamification. These features provide a solid and unique framework for collecting citizen-science data on single trees.

1. Introduction

Trees, as the main component of the terrestrial carbon sink, offer a nature-based solution for removing anthropogenic carbon from the atmosphere by absorbing carbon dioxide and locking up carbon. Despite this important function, the quantification of global tree biomass, i.e., the carbon stored in trees, is still challenging (Araza et al., 2022; Pan et al., 2024; Santoro et al., 2021) where the estimation of the uptake

* Corresponding author.
E-mail address: milenkovic@iiasa.ac.at (M. Milenković).

https://doi.org/10.1016/j.ecoinf.2026.103897
Received 11 August 2025; Received in revised form 19 June 2026; Accepted 19 June 2026
Available online 22 June 2026

of carbon by land in the global carbon cycle currently has the highest uncertainties (Friedlingstein et al., 2023). One component contributing to this highly uncertain biomass quantification is tree populations that are outside of forests, which can often accumulate more than 10% of the national aboveground biomass (Liu et al., 2023; Schnell et al., 2014). Beyond carbon storage, trees outside forests have an economic value for different local communities involved in agroforestry (Pantera et al., 2018), as well as providing wind protection for crops and snow management for fields and roads in rural areas (Smith et al., 2021), whereas urban trees positively affect the microclimate of cities (Wang et al., 2015). Quantification of single trees enables them to be better managed and is thus relevant for all these applications.

There are several established workflows for the collection of carbon-relevant tree data within forests (Table 1). For instance, national forest inventories (NFI) collect data typically from a systematic spatial and temporal sampling of forests with a set of permanent plots, where single tree measurements such as the diameter at breast height (DBH), tree species identification, tree height (TH), etc. are collected and can be used to estimate forest aboveground biomass (AGB) and carbon. These measurements are typically acquired with forestry tools such as a caliper or a diameter tape, a laser range finder, and a Global Navigation Satellite System (GNSS) receiver (Pereira et al., 2019). Such a systematic, rigorous, and well-planned collection of measurements is reliable and statistically stable over time, e.g., with respect to comparability between different acquisition times, but also labor-intensive to maintain over large areas (McRoberts et al., 2010). Moreover, NFI data are typically not open, or for specific countries, not fully open, as their exact geolocation is not shared to avoid arbitrary visitors entering the plots and compromising their representativeness in the NFI sample (Schadauer et al., 2024). To improve the accuracy of the biomass estimates over large areas, ground measurements are typically combined with remote sensing data such as multispectral images, airborne and space LiDAR (Light Detection And Ranging), or space RADAR (Radio Detection And Ranging) data that offer full coverage over large areas (Kangas et al., 2018; Magnussen et al., 2018; Saarela et al., 2015). Trees outside the forest are also inventoried, but in ways that differ from national forest inventories, given their distinct management objectives and benefits. Urban tree inventoriesinventory, for example, shall include a number of attributes to enable assessments of public safety, conflicts with built infrastructure, and different ecosystem services such as carbon sequestration and air-pollution removal, etc. (Roy et al., 2012). These diverse objectives are also reflected in an increased measurement and estimation variability compared to NFIsNFI (Westfall et al., 2021). In addition to basic dendrometric attributes, urban inventories commonly capture canopy structure attributes, such as cover, density, width, and height, because of their relevance to urban tree functions, such as microclimate regulation, noise attenuation, etc. (Smithers et al., 2018; Zhao et al., 2021). These attributes can be collected through conventional field measurements using standard inventory tools, such as diameter tape, caliper, hypsometer, etc. (van Doorn et al., 2020), and can also be derived from remote sensing measurements, including laser scanning (Saarinen et al., 2014) and street or aerial images (Li et al., 2019; Lumnitz et al., 2021). We focus here on measuring carbon-related attributes such as total tree height, stem diameter, and tree species.

Ground measurements of single trees have also been collected using other surveying methods, such as laser scanning. Terrestrial laser scanning (TLS) instruments transmit laser pulses at regular zenith and azimuth angle increments from the standing position and record the double travel time and intensity of the backscattered laser energy, which is used to produce a three dimensional (3D) point cloud, i.e., a collection of 3D points of the scanned environment such as tree stems, leaves, branches, understory vegetation, and any other object in the scene (Vosselman and Maas, 2010). These georeferenced point clouds also serve as the basis for extracting single-tree or plot-level attributes, either manually or automatically (Liang et al., 2018). In addition to individual attributes, more complex tree structures, such as stem curves and even complete 3D tree volume models (including branches) can be derived from TLS point clouds (Lau et al., 2018; Liang et al., 2014; Raumonen et al., 2013) and converted to nondestructive AGB estimates. TLS can provide information about single trees rapidly and accurately at the plot level, but it also requires multiple scan positions per plot to minimize occlusions, which reduces the efficiency of this approach over large areas. Furthermore, due to scanning from the ground, treetops can be occluded and therefore result in the underestimation of tree height (Liang et al., 2018). Laser scanning from an unmanned aerial vehicle (UAV) flying over the forest canopy acquires point clouds with a good representation of both the treetop and the ground and thus, provides more accurate estimates of tree height than TLS while covering larger areas (Brede et al., 2017). Nevertheless, laser scanning equipment is expensive, and tree and plot-level attributes are not measured directly but are instead derived from point clouds relying on specialized software and expert processing such as georeferencing, co-registration, noise reduction, and dealing with data artefacts, such as ghost points when scanning branches under windy conditions (Liang et al., 2016; Liang et al., 2019).

Terrestrial photogrammetry is an inexpensive alternative to laser scanning that uses overlapping images acquired with consumer-grade cameras and structure-from-motion methods to produce plot-level point clouds (Iglhaut et al., 2019). Different plot image acquisition settings have been tested from multiple cameras attached with fixed horizontal and vertical bases and acquisitions from a single standing point, e.g., the plot center (Forsman et al., 2016); two cameras with a fixed vertical base attached to a stick with a GNSS receiver and stop-and-go acquisition along a predefined route (Liu et al., 2018); and a hand-held single-camera image acquisition while walking through the forest plot (Mokroš et al., 2018; Piermattei et al., 2019). The accuracy and

Table 1
An overview of single-tree forest and outside forest ground data collection approaches and their characteristics. "Operationally in use" refers to whether the approach is currently being used operationally in national forest monitoring. Costs are just rough descriptive estimates of the expenses associated with equipment, processing software, and personnel hours. That information is based on the authors' knowledge and understanding of the field. Supporting literature is cited where available.

	Operationally in use	Single tree information	Stand characteristic acquired	Statistically planned sampling	Expert knowledge required	Costs
Forest Inventory (FI)	Yes	Directly measured	Yes	Yes	Yes	High
Terrestrial laser scanning (TLS)	No[1]	Indirectly derived from point clouds	Yes	Yes	Yes[2]	High
Terrestrial Photogrammetry	No	Indirectly derived from point clouds	Yes	Yes	Yes[2]	Medium[3]
Citizen-Science with Mobile Phones	No	Directly measured in the app	No	No	No	Low

[1] Except for a few countries, e.g., France, Finland, Switzerland, and Sweden, that experimented with integrating TLS into their national forest inventories (Holvoet et al., 2025; Kükenbrink et al., 2025; Persson et al., 2022).
[2] Particularly for the data post-processing and information extraction phases.
[3] The costs of the equipment are low, but the software and postprocessing costs can be medium to high.

completeness of the reconstruction depend primarily on the image quality but also on the number of images, which may affect the method's efficiency. Although some studies have demonstrated that the number of images can be reduced (Mulverhill et al., 2019), tree- and plot-level attributes are not measured directly but are derived from image-based point clouds, relying on specialized software, expert processing, and additional distance or geolocation measurements to rescale image-based point clouds.

A more recent approach to provide direct, inexpensive, and efficient single-tree measurements is through using mobile phones, which can integrate geolocation, orientation, and imaging sensors, such as GNSS receivers, accelerometers, gyroscopes, cameras, and sometimes LiDAR (Magnuson et al., 2024). There are three main types of smartphone-based data acquisition methods: passive sensing, active sensing, and combined techniques (Magnuson et al., 2024). Passive sensing relies primarily on the smartphone's built-in RGB cameras to capture images or videos, which are then processed using photogrammetric techniques such as Simultaneous Localization and Mapping (SLAM) to extract spatial information. These methods often incorporate data from additional sensors, such as the accelerometer and gyroscope, to allow scaling and support constraining the SLAM results. Commonly used software development kits (SDKs) in this context are Google's ARCore (Lanham, 2018) and Apple's ArKIT (Buerli and Misslinger, 2017), which both support real-time motion tracking and environmental understanding without requiring external hardware, leaving them usable for most smartphones on the market. For example, 90% of active Android devices support ArCore as of November 2024 (Google, 2025).

By carefully moving the smartphone while pointing the camera at a tree, depth maps of the trunk can be estimated. This depth map holds information about the sensor-trunk distance and allows for metrical information. In recent years, several studies have been published exploiting the AR (augmented reality) functionality of these SDKs to tailor bespoke tree parameter measurement apps. Many recent apps provide the possibility to measure tree parameters that fundamentally rely on ArCore or ArKit. Examples of these apps are: Working Trees (Ahamed et al., 2023), ARTreeWatch (Wu et al., 2023), and GreenLens (Feng et al., 2024).

The NASA GLOBE (Global Learning and Observations to Benefit the Environment programme) Observer app represents a special case of passive sensing and does not rely on advanced spatial processing algorithms (Amos et al., 2020). Instead, it estimates tree height using a trigonometric method based on the smartphone's built-in gyroscope and accelerometer. Users are instructed to point the device at the base and top of the tree to measure angles from a distance and then walk in a straight line towards the tree while counting their steps to estimate distance. The user's body height is entered and used to approximate step length, which is factored into the height calculation.

In contrast, active sensing technologies rely on smartphones equipped with emitting sensors to capture spatial information from the surrounding environment. Early attempts to integrate active sensors for smartphone-based tree parameter estimation were made through Google's Tango project, which incorporated a near-infrared depth sensor into smartphones. Tango was successfully tested for estimating tree parameters (Hyyppä et al., 2018; Tomaštík Jr. et al., 2017), but the project was discontinued by Google in 2017 (Matney, 2017). Today, active sensing with smartphones involves devices equipped with LiDAR sensors or Time-of-Flight (ToF) cameras, as seen in recent iPhone, iPad, and mid- to high-end Android models, such as the Samsung Galaxy S20+ and S20 Ultra, the Huawei P40 Pro+, and the Sony Xperia Pro—I. Several studies have explored the potential of combining these sensor-equipped devices with custom applications to measure tree attributes such as DBH and basal area (e.g., Bobrowski et al., 2023; Çakir et al., 2021; Pace et al., 2022). However, estimating TH with active sensing alone remains challenging due to the limited range of these sensors. For example, the widely used iPhone 12 Pro has a maximum LiDAR range of approximately 5 m (or 10 m for the iPhone 16 Pro), which is insufficient for capturing the height of mature trees (Luetzenburg et al., 2021).

Finally, combined sensing methods leverage both active and passive sensor data to enhance spatial understanding. By integrating information from multiple sensors, these approaches generally produce more accurate and reliable results. The limitations of both active and passive sensors can often be mitigated through their complementary use. For example, the low granularity of ToF-based depth maps can be mitigated by incorporating high-resolution RGB imagery, which improves trunk segmentation, a crucial step in DBH estimation (Feng et al., 2024). ARCore and ArKIT are designed to implicitly incorporate active sensors like ToF cameras into their depth estimation processes. This integration makes them a practical solution for enabling spatial sensing capabilities across a broad range of smartphones, from low- to high-end models. Thus, most current apps, including the apps listed above, support both passive and combined sensing methods if the smartphone used is equipped with the necessary sensors.

In contrast to expert ground data collection for forestry and biodiversity monitoring, there are also mobile apps targeted at citizen science, with the goal of providing crowdsourced data streams to complement satellite and expert data. For example, Ferster and Coops (2016) acquired and combined crowdsourced data on forest fuel attributes with high-resolution satellite images to map forest structural components over a large area. They used a mobile phone questionnaire to interview volunteers and asked them to visually interpret tree and plot attributes, such as the crown base height, stem density, understory conditions, crown closure, etc. Crowdsourced data from apps such as Pl@ntNet and iNaturalist, which use automatic visual identification of plants from mobile phone images, have proven to be reliable data sources for ecological monitoring and biodiversity (Bonnet et al., 2020; Di Cecco et al., 2021). Within its GLOBE programme, as mentioned above, NASA has engaged with students and citizens worldwide through its GLOBE Observe smartphone app to collect different crowdsourced ground data (Amos et al., 2020). The Tree module, in particular, has been designed to acquire tree height measurements and support the interpretation of tree height measurements acquired with the Ice, Cloud, and land Elevation Satellite-2, ICESat-2 (Enterkine et al., 2022). As discussed by Neuenschwander et al. (2024) and Duncanson et al. (2022), crowdsourced single-tree heights can support AGB mapping based on the ongoing space-borne LiDAR missions from NASA, such as ICESat-2 and GEDI.

These studies demonstrate the considerable potential and demand for citizen science and crowdsourced single-tree data for mapping tree biomass and carbon storage. However, due to its heterogeneous data quality, crowdsourcing requires additional procedures to improve data consistency and exclude low-quality measurements (Roman et al., 2017; See et al., 2013). Although novel AR-based apps for carbon-related measurements are freely available, crowdsourcing with them is not straightforward because they lack data-quality curation procedures and an integrated database to support user engagement. The latter is particularly important for gamification with AR apps that affect user engagement in urban forestry data collection campaigns (Chambers et al., 2025). Furthermore, crowdsourcing with those apps requires an additional app for tree species identification, which unnecessarily complicates the citizen measurement workflow and the integration of all citizen measurements into a single database.

Here, we present a crowdsourcing-ready workflow that includes a novel, freely available citizen-science mobile app, Tree-Quest, that uses AR to measure single-tree attributes, such as DBH and TH, integrates the Pl@ntNet API for tree species identification, and a crowdsourced data quality curation step based on the Tree-Quest AR image labeling with a PicturePile (Danylo et al., 2018; Fraisl et al., 2022) extension additionally customized for this task. This freely available workflow enables citizens and experts to collect carbon-related single-tree measurements, thereby providing an open, crowdsourced data stream for mapping forest biomass and vegetation carbon storage. The main advantages of Tree-Quest compared to existing apps are that it:

- integrates in one survey the collection of the three most important tree attributes: DBH, TH, and tree species,
- can be customized by initiating specific quests tailored to the needs of different user groups, e.g., scientific experts, forest owners, and citizens,
- collects auxiliary images with AR objects for assessing the quality of the citizen data in post-processing,
- has an open data portal to present and explore the data collected with the app,
- supports citizen engagement through gamification with the user leaderboard integrated into the data portal,
- is freely available for both Android and iOS phones and can work with phone images only, i.e., no LiDAR sensor is required on the phone

The paper is organized as follows. We begin with a description of the functionalities and underlying methods employed in the app, followed by a description of the test sites, data, and methods used to perform a quantitative assessment of measurement accuracy that is presented in the results. Finally, we discuss the app's advantages and limitations, provide major recommendations for its usage, and conclude. The app's accuracy is calculated based on differences from DBH and TH measurements: (a) obtained with tools used in a traditional forest inventory (FI) survey, and (b) derived from TLS point clouds. We take advantage of Tree-Quest's ability to store screenshots with AR objects to perform data curation and analyze how volunteers' measurement quality affects DBH and TH accuracy. The Tree-Quest measurements are also compared with those collected by other mobile apps.

2. Crowdsourcing workflow with Tree-Quest

The crowdsourcing-ready workflow (Fig. 1) includes the following three components: (a) our app Tree-Quest for carbon-related single tree attribute measurements, (b) its data portal that supports data download and currently only basic gamification through different leaderboards, and (c) quality labeling of Tree-Quest measurements through Tree-Quest screenshots, i.e., a pile, provided to a customized PicturePile extension for their classification.

Tree-Quest (TQ) is a free citizen science tool for measuring single-tree attributes. It allows any volunteer to use it to survey trees with their smartphone at any location and at any time. TQ is available as a quest (or what is essentially a citizen-science campaign) within Geo-Quest, a broader mobile app developed by the International Institute for Applied System Analysis (IIASA), which contains a range of quests on diverse topics such as identifying land-cover change, crop types, etc. (Fig. 2a). TQ integrates modules for automatic and manual DBH measurements, TH measurements, tree species identification, and a questionnaire about each measured tree.

TQ's TH and DBH modules are built as interactive 3D AR

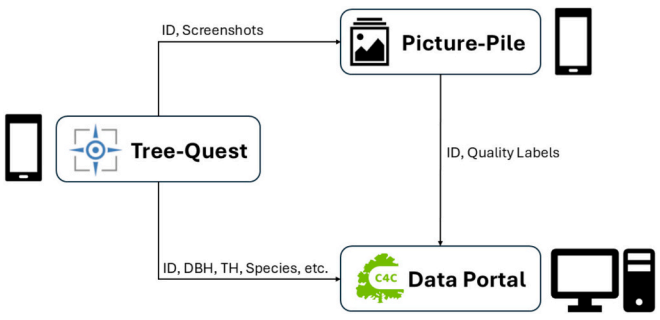

Fig. 1. Crowdsourcing-ready workflow that includes Tree-Quest app for carbon-related single tree attribute measurements, PicturePile for quality labeling of crowdsourced data, and a data portal for user engagement, data download, and presentation.

environments. The single-tree measurements are based on user input and 3D points, i.e., feature points, provided by the off-the-shelf AR solutions for Android and iOS phones: the ARCore (Lanham, 2018) and ARKit libraries (Buerli and Misslinger, 2017), respectively. The modules render feature points and provide a tool and instructions for the user to manually select one feature point from which all relative measurements are derived later (Fig. 2e). This so-called *seedpoint* defines the horizontal and vertical planes in which the DBH and TH are calculated, respectively. Two approaches are implemented for the DBH measurements: automatic and manual.

The automatic DBH approach does not require user input; it automatically selects all feature points within a vertical buffer centered on the horizontal plane (the red points in Fig. 2f). Additional points are then added to the selection only if the horizontal distance to their nearest neighbor in the already selected feature points is: (a) larger than a minimal allowed distance threshold, or (b) smaller than a maximal allowed distance threshold. The default values are set empirically to 3 cm for the vertical buffer height and the 3 cm minimal distance, and 20 cm for the maximal distance, but the values can also be changed through the settings in the expert mode (Fig. 2h). The parameters are introduced to control the density of selected points and filter out potential outliers. The selected points are used to fit a circle in the horizontal plane. The diameter and area of the circle are stored as the DBH and the basal area of the measured tree, respectively. It is noted that for inclined trees, DBH could be slightly overestimated as the circle fit is always in the horizontal plane.

The manual DBH approach renders a vertical line as an AR object and asks the user to align it to the left and then to the right side of the tree to record the 3D vectors from the observation point to each side. Following simple rules of geometry, these vectors and the seedpoint coordinates are then used to calculate the DBH and the basal area. Manual and automatic DBH measurements are called circular and angular methods, respectively. After any of them is utilized, the app also records a screenshot with the AR circle rendered over the tree, allowing for measurement quality assessment in a potential data curation post-processing step.

TH is measured manually; the app renders a crosshair as an AR object and asks the user to point at the bottom and top of the tree (Fig. 2g). The vertical distance between the intersection points of the top and bottom 3D vectors with the vertical plane is stored as TH. As it can rely only on camera observations, there is no ToF maximal distance constraint, and the user can take a longer distance apart from the tree to perform the treetop measurement. While doing this, it is, however, important to keep the phone camera oriented towards the tree to avoid breaking the AR session. In contrast, when the treetop is measured not far away from the tree, i.e., with a phone inclination of more than 45 degrees, the user receives a warning, but the measurement is stored. After the TH measurement is performed, the app records a screenshot with the AR cylinder rendered to support potential data curation.

The tree species module for species identification is based on the Pl@ntNet API (Pl@ntNet, 2025). The user is asked to take a photo of a tree and send it to Pl@ntNet for identification (Fig. 2c). The app also allows users to take photos of specific tree organs, such as leaves, flowers, fruits, bark, or an overview photo with auto-identification, and to repeat the identification process with additional photos (Fig. 2d). The first 10 species returns from the Pl@ntNet AI model, i.e., predicted tree species names with their associated probabilities, are presented to the user in a dropdown menu for final tree species selection (Fig. 2c).

A single tree is measured with TQ through the following steps. First, a user must register and create an account in the Geo-Quest app. The user then selects the TQ module from GeoQuest's main menu (Fig. 2a). TQ starts with a screen containing a brief description of the campaign. A base map is shown on the next screen, and the user is asked to tap on it to locate a tree on the map (Fig. 2b). On the next page, the user is asked to enter the name of a tree to identify it more easily in the database later (Fig. 2c), take a photo (Fig. 2d), and select the tree species based on the

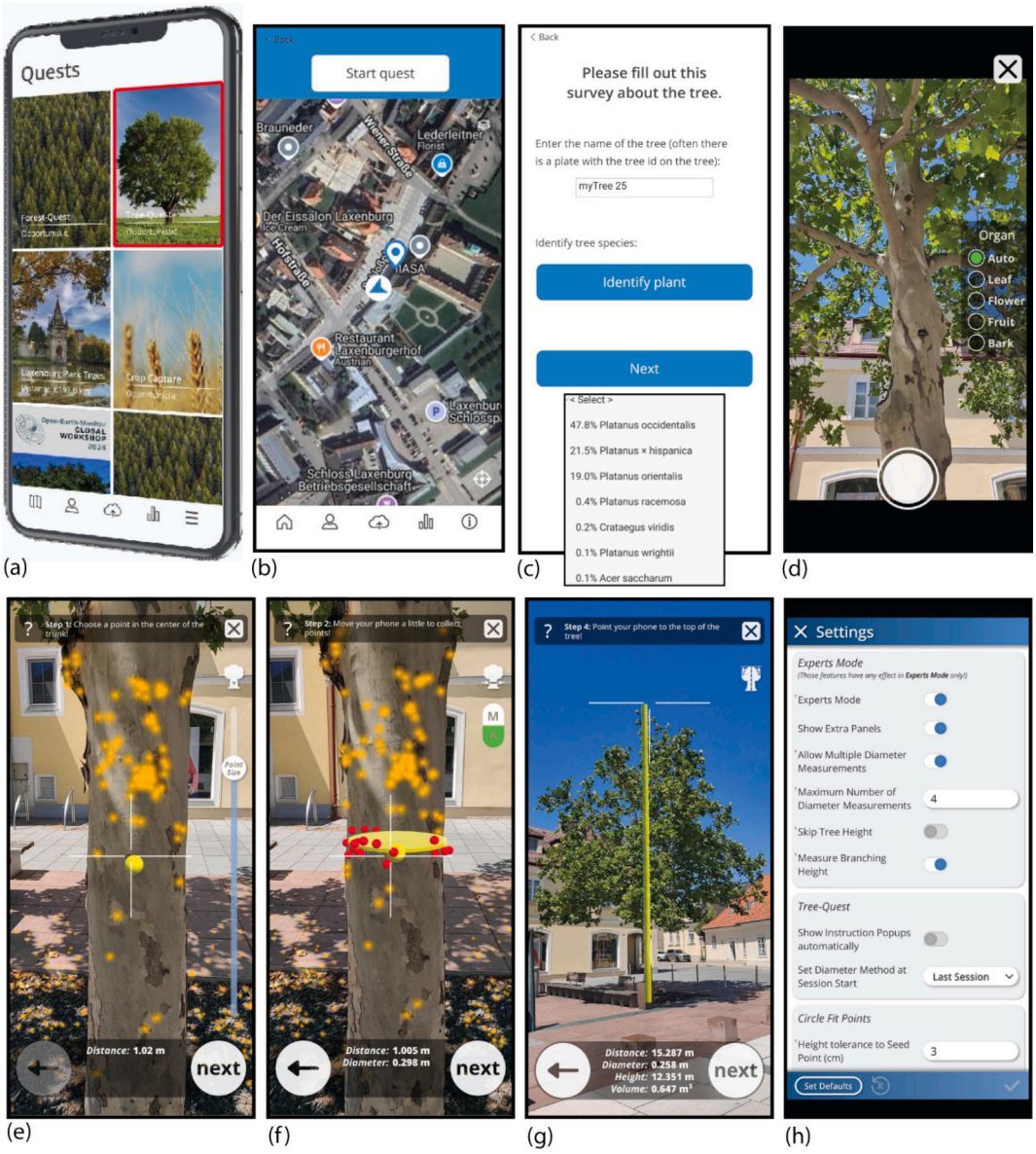

Fig. 2. Tree-Quest main modules and their screens: (a) the Geo-Quest main menu with the Tree-Quest entry point highlighted with the rectangle, (b) the screen with a base map to digitize the location of the tree and start the quest, (c) a screen with an access button to tree species identification with a list of outputs coming from the Pl@ntNet API, (d) a screen to collect an image for tree species identification with different options, (e) a screen showing the selection of the seed point the only (larger bright yellow point) among all feature points, (f) a screen with a circle fit for deriving the tree diameter based on the selected (red) feature points, (g) a screen for tree height measurement, (c) a screen for the expert mode settings. (For interpretation of the references to colour in this figure legend, the reader is referred to the web version of this article.)

responses offered by Pl@ntNet (Fig. 2c). The user is further instructed to select a seed point at approximately 1.3 m above the tree bottom, i.e., at the so-called breast height, to provide a diameter measurement following forest inventory standards (Fig. 2e). Once completed, the user is asked to measure the DBH using the automatic or manual method (the A and M buttons in Fig. 2f). The user is then asked to measure the TH (Fig. 2g). Finally, the user fills out a questionnaire about the tree, specifying whether it is natural, planted, damaged, or answering any additional questions relevant to the campaign. The questionnaire can be redesigned to meet the specific needs of a campaign. Upon completing the quest (i.e., the single-tree measurement), the user can then upload the data collected to the Geo-Quest server.

Geo-Quest, including the TQ module, is available for free on the Google Play Store for Android phones and the App Store for iOS phones. The TQ data uploaded to the Geo-Quest server are open and available to any registered user, and they can be explored and downloaded from the Citizens for Copernicus (C4C) data portal: https://c4cweb.main.geo-wiki.org. The portal also displays data from other single-tree campaigns (quests) in Geo-Quest.

The crowdsourced-ready workflow will then require an additional quality curation for the acquired crowdsourced data. Therefore, we introduced a quality-labeling step in which the quality of each DBH or TH measurement is assessed by labeling TQ screenshots that contain either a fitted circle or a cylinder captured during the measurement. The screenshots are labeled in our existing app, PicturePile, which we slightly adapted so that a user can simply move an image in one of four directions to label it in one of the following categories: high, medium, low, or other (see Fig. 3). The labeling in PicturePile is very simple, allowing a rapid image labeling, which has already shown its usability for crowdsourcing through image interpretation (Danylo et al., 2018; Fraisl et al., 2022). The labeling in this study was performed by two experts. When the labels disagreed, the lower-quality category was

Fig. 3. PicturePile user environment adapted for manual labeling of the TQ screenshots with AR objects into one of the quality categories: high, medium, low, and other ("CantCan't tell"). The labeling is done by manually moving the TQ image in one of the four directions. A labeling of TQ diameter measurement with medium-quality score is shown in (a), and a labeling of TQ tree height measurement with low-quality is shown in (b).

taken as the final one. The "other" category included cases where it was not possible to judge the quality, or when an apparent measurement error was evident, e.g., when a screenshot was missing, the AR object was partially or not visible at all, or the AR object size was erroneous.

3. Materials and methods

The TQ measurements of DBH and TH were collected, processed, and compared with measurements obtained with forest Inventory (FI) tools, terrestrial laser scanning (TLS), and other apps for DBH and TH measurement. Fig. 4 shows the major data and processing steps applied, and subsequent sections explain them in detail.

3.1. Test sites

Two test sites were introduced to assess the app's accuracy and gain user feedback: Laxenburg Park and Stadtpark in Vienna, both in Austria. The Laxenburg Park test site comprises 45 trees that are part of a 2.8 km^2 heritage-protected palace landscape garden located near Vienna in Laxenburg. The trees were selected to be close to the park's main entrance to maximize citizen participation (Fig. 5a). All the trees were originally planted, with current DBH values ranging from 11.9 cm to 161.2 cm and THs ranging from 4.6 m to 29.0 m. Tree species were diverse, coming from 11 genus groups, but predominantly including *Tilia, Celtis, Acer, Platanus, Aesculus,* and *Pinus* species. In particular, there were several *Platanus Orientalis*planetrees with a DBH over 100 cm, which were challenging to measure. The trees were planted sparsely, visible from the side, and most of them have no understory except for a few with basal shoots and small bushes around them. In addition to the citizen measurements taken with the TQ app, the trees were surveyed using forest inventory tools and TLS, which were employed here to assess the app's accuracy and provide

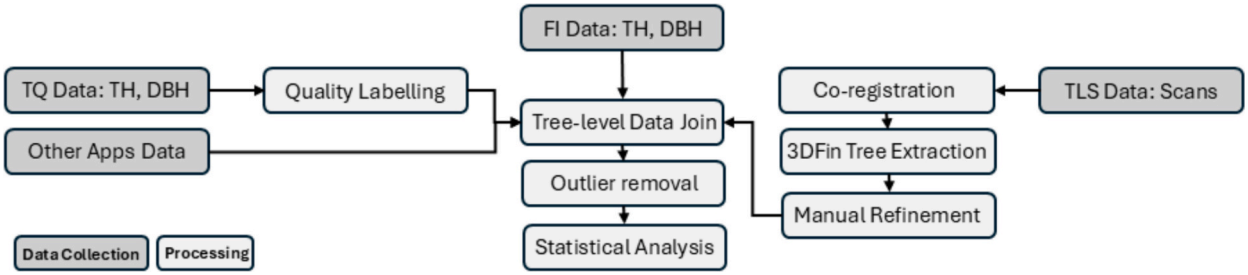

Fig. 4. An overview of data collected, and processing steps applied for assessing TQ measurements' accuracy.

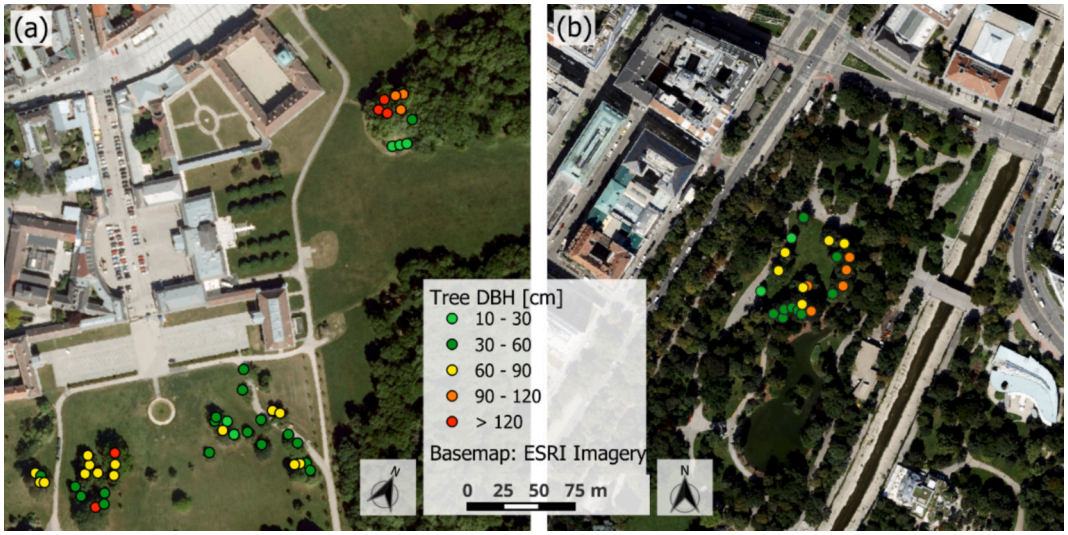

Fig. 5. Locations of the trees surveyed in (a) the Laxenburg Park test site (N 48° 12′ 21“, E 16° 22’ 50”), and (b) the Stadtpark test site (N 48° 3′ 58.233“, E 16° 21’ 36”). The tree colour corresponds to the DBH group marked in the legend.

recommendations for future app usage. An ecology expert collected the forest inventory measurements.

The Stadtpark test site includes 22 trees clustered in one part of an urban park located centrally in Vienna (Fig. 5b). Only trees with minimal or no crown overlap with neighboring trees were considered to minimize measurement ambiguities. The trees were originally planted and had DBHs ranging from 19.8 cm to 116.9 cm, and THs ranging from 9.0 m to 21.0 m. Tree species were diverse, coming from 11 genus groups, predominantly including *Acer, Fagus, Pinus, Quercus*, and *Aesculus*. This test site was surveyed by experts only (not citizens) using various forestry mobile apps, referenced against forest inventory measurements. The data collected in Stadtpark were used to compare TQ DBH and TH measurements with other apps.

3.2. Single-tree inventory data

Single-tree inventory data include DBH and TH measurements that were collected consistently using traditional FI tools and methods for each of the 67 trees (45 and 22) across the two test sites, i.e., the FI-DBH and FI-TH measurements. DBH was measured at 1.30 m above ground level using a 5 m diameter tape (Grube-Forst GmbH, n.d). For the evaluation of TH, a laser rangefinder was used to triangulate following the tangent method (Larjavaara and Muller-Landau, 2013). The FI measurements were collected by a forest ecology expert who also carried out the identification of the tree species. The FI-DBH and FI-TH measurements were used to assess the relative accuracy of the corresponding TQ and TLS measurements.

3.3. DBH and TH from TLS data

Single-tree DBH and TH were additionally acquired in Laxenburg Park using TLS. For the TLS campaign, a RIEGL VZ-600i scanner was used. It features a beam divergence of 3.5 mrad, resulting in a 3.5 cm increase in beam diameter per 100 m. The documented 3D point accuracy is 3 mm at 50 m and 5 mm at 100 m. A pulse repetition rate of 2.2 MHz was used, with an angular spacing of 0.034 degrees, corresponding to a sampling interval of ~6 cm at a distance of 100 m. Data collection took place just before the onset of foliage on 22 March 2024. Wind was minimal during the campaign. Overall, the scanning conditions were favorable. The three locations on which trees in the test site clustered (Fig. 5a) were scanned and processed individually, with 10 to 40 scan positions, depending on the location size. Co-registration of the scans was performed using RiSCAN PRO software (v. 2.19.1) and yielded an accuracy of 0.009 m for the average standard deviation over all scan positions. The resulting co-registered point clouds were then used for semi-automatic estimation of DBH and TH. For this, the software 3D Forest Inventory (3DFin) was used (Laino et al., 2024). 3DFin is a Python-based plugin for the point cloud processing software CloudCompare (v.2.13.0). The resulting DBH and TH estimates were manually checked and measured again if necessary. The estimation of DBH consistently yielded good results with little to no visible deviations between the fitted circle and the point cloud. The automatic TH estimation tended to be less accurate, particularly for dense tree clusters that featured trees with complex topologies. These trees were then manually remeasured using the measurement tool implemented in CloudCompare. This process resulted in a highly accurate reference dataset for quantitatively evaluating the performance of the TQ app.

3.4. DBH and TH from Tree-Quest

On both test sites, single-tree DBH and TH measurements were collected with the TQ app. For Laxenburg Park, 30 volunteers made 681 measurements of the 45 trees, resulting in 10 or more measurements collected per tree.

To assess the measurement quality among different volunteers, they were split into three groups: experts, practitioners, and students. The groups were formed according to the volunteers' familiarity with the TQ app. The experts were the smallest group, comprising four volunteers who participated in the app's development and/or had tested the app intensively beforehand. The practitioners involved six volunteers who were familiar with the app but had not used it before. They were project partners in developing the app. Finally, the students were the largest group, which included 20 volunteers who were unfamiliar with the app and had not used it before. This group was formed from participants in the GEO-OPEN-HACK-2024 hackathon, who were mostly PhD students and early-career researchers. Despite the apparent imbalance in the number of volunteers per group, the number of measurements per group was more balanced, i.e., 278, 231, and 172 measurements from the experts, practitioners, and students, respectively.

The above groups were given the same instructions for the measurements, except for the number of trees to be measured. Students were instructed to freely select which tree and how many trees they would like to survey in Laxenburg Park. Furthermore, they could freely select manual or automatic DBH methods. The practitioners received the same instructions as the students but were required to measure at least 30 trees. Finally, the experts had the same instruction as the students and

practitioners, but they had to measure each tree using both DBH methods. All groups were advised to make DBH measurements at approximately 1 to 2 m from the tree and at a tree height of 1.3 m. For measurements of TH, we advised the volunteers to move approximately one tree height away from the tree to obtain a better angle of view of the treetop.

Each TQ DBH and TH measurement was also classified into one of the following quality categories: high, medium, low, and other. The classification was done independently by two experts, who visually inspected each TQ screenshot acquired by the app during different phases of the measurement. The screenshots display the augmented reality objects (a circle and a cylinder for DBH and TH inspection, respectively) as well as the measured tree, which was used to visually assess the measurement quality. As a result, each measurement was scored twice using the above quality categories. When the labels disagreed between the two experts, the lower quality category was taken as the final one. The "other" category included cases where it was not possible to judge the quality or when an apparent measurement mistake was visible, e.g., when a screenshot was missing, the AR object was partly or not visible at all, or when the AR object size was erroneous. The DBH and TH measurements from the "other" category were excluded from the analysis.

The high-, medium-, and low-quality categories also contained outliers when compared with the FI measurements. These were mostly correct but were assigned to the wrong tree erroneously. This probably happened because an incorrect tree number was entered by a user at the beginning of a tree measurement session. We excluded these measurements based on interquartile range outlier detection and moved them to the "other" category, i.e., they were excluded from the analysis.

For Stadtpark, the TQ DBH and TH measurements were only compared with other forestry mobile apps. One expert collected the TQ TH and DB measurements for each of 22 trees. The expert also collected the DBH and TH measurements using the other forestry apps for comparison. The measurements from each app were also first filtered for outliers before the subsequent analysis.

We created several data subsets from Laxenburg Park and Stadtpark TQ data to evaluate different mobile app quality aspects. Table 2 lists these subsets and their usage in the subsequent analysis.

Table 2
Overview of Tree-Quest data subsets and their characteristics from the Laxenburg Park (LP) and Stadtpark (SP) test sites, including their description and usage in the subsequent analysis.

Data Subset	Description	Number of Meas.	Derived from	Usage	Test site
All-LP	All DBH and TH measurements in Laxenburg Park	681	–	–	LP
H	High-quality DBH and TH measurements	DBH: 98 TH: 52	All-LP	Sections 4.1, 4.2, and 4.4	LP
M	Medium-quality DBH and TH measurements	DBH: 228 TH: 254	All-LP	Section 4.2	LP
L	Low-quality DBH and TH measurements	DBH: 117 TH: 148	All-LP	Section 4.2	LP
HM	High- and medium-quality DBH and TH measurements	DBH: 326 TH: 306	H + M	Section 4.2	LP
HML	High-, medium-, and low-quality DBH and TH measurements	DBH: 443 TH: 454	H + M + L	Section 4.2	LP
E	DBH and TH measurements acquired by experts	DBH: 155 TH: 220	HML	Section 4.3	LP
P	DBH and TH measurements acquired by practitioners	DBH: 187 TH: 154	HML	Section 4.3	LP
S	DBH and TH measurements acquired by students	DBH: 101 TH: 80	HML	Section 4.3	LP
Man	High-quality DBH measured with the manual (angular) method	DBH: 76	H	Section 4.4	LP
Auto	High-quality DBH measured with the automatic (circle fit) method	DBH: 22	H	Section 4.4	LP
All-SP	All DBH and TH measurements in Stadtpark	DBH: 18 TH: 22	–	Section 4.5	SP

3.5. DBH and TH from other apps

To understand how TQ measurements compare with other existing apps, we conducted single-tree DBH and TH measurements in Stadtpark with TQ and additional tree apps: Working Trees, GreenLens, and GLOBE Observer. Working Trees measures DBH and TH, whereas GreenLens measures only DBH, and GLOBE Observer only TH. Thus, for each tree, we obtained one DBH and one TH measurement using the TQ app, and two additional DBH and TH measurements using the aforementioned apps. We wanted to consider only free apps, including those that rely on both similar and different measurement technology compared to TQ. For example, GLOBE Observer measures the inclination angle of a phone and uses the number of steps entered by a user to calculate the TH. In contrast, Working Trees interactively asks the user to measure TH from the tree's bottom to the top, relying on the phone's AR, which is very similar to TQ TH measurements. For DBH, both apps rely on the phone's AR; however, GreenLens derives DBH automatically with AI-supported tree width detection, i.e., without requiring the user to interactively measure it, which is also the case for Working Trees. The characteristics of the selected apps are given in Table 3. All app measurements were conducted on April 1, 2025, by the same user.

3.6. Statistical analysis

The TQ DBH and TH relative accuracy was assessed with a linear model between TQ measurements (Table 2) and the counterpart FI measurements (Sections 3.2). We applied linear mixed-effects models with random intercepts by individual tree to account for within-tree clustering of multiple TQ submissions. The model performance was reported with its coefficient of determination (R^2):

$$R^2 = 1 - \frac{\sum_{i=1}^{n} \left(y_{TQ,i} - \hat{y}_i\right)^2}{\sum_{i=1}^{n} \left(y_{TQ,i} - \bar{y}_{TQ}\right)^2}$$

where $y_{TQ,i}$ is a TQ measurement, $\hat{y}_i$ is the predicted value, and $\bar{y}_{TQ}$ is the mean of the $y_{TQ,i}$ values. The calculations were done with the Python statsmodels library (Seabold and Perktold, 2010).

In addition, the mean absolute error (MAE) and the relative mean absolute error (rMAE) were calculated with respect to the FI measurements:

$$MAE = \frac{1}{n}\sum_{i=1}^{n}\left|y_{TQ,i} - y_{FI,i}\right|, \text{ and } rMAE\,[\%] = \frac{1}{n}\sum_{i=1}^{n}\left|\frac{y_{TQ,i} - y_{FI,i}}{y_{FI,i}}\right| \bullet 100$$

where || is the absolute operator, $y_{TQ,i}$ is a TQ measurement, $y_{FI,i}$ is an FI measurement, and n is the number of measurements. It is noted that our MAE and rMAE were influenced by both bias and precision, as the model was not considered in their calculations.

To relate the results more easily with other studies, we also calculated and reported the root mean square (RMSE) with respect to the FI measurements:

$$RMSE = \sqrt{\frac{1}{n}\sum_{i=1}^{n}\left(y_{TQ,i} - y_{FI,i}\right)^2}$$

Table 3
Overview of the apps from which the TH and DBH measurements from Stadtpark were collected and used for the comparison.

Name	Operating system	Tree Parameters	AR Supported	Measurements	Phone used	Reference
GLOBE Observer	Android, iOS	TH	No	Manual	OnePlus6 (Android)	Campbell (2021)
GreenLens	Android	DBH	Yes	Automatic (AI-supported)	Samsung Galaxy M34 (Android)	Feng et al. (2024)
Working Trees	iOS, Android	TH, DBH	Yes	Manual	Samsung Galaxy M34 (Android)	Ahamed et al. (2023)
Geo-Quest	Android, iOS	TH, DBH	Yes	Manual and Automatic	OnePlus6 (Android)	This publication

To compare TQ with TLS and other apps, we calculated the accuracy metrics (R^2, MAE, and rMAE) by substituting measurements from TLS or other apps into the above equations instead of the TQ measurements. The metrics were calculated separately for DBH and TH measurements. A larger R^2 indicates a better fit with the FI measurements, whereas smaller MAE and rMAE indicate better accuracy. The linear model coefficients (slope and intercept) show the nature of bias in the measurements.

To understand if the TQ, FI, and TLS measurements are statistically interchangeable, we assessed bias among them and tested their significance. The bias (B) was calculated as the median of the difference between the TQ measurements ($y_{TQ,i}$) and FI measurements $\left(y_{FI,i}\right)$ and it is also expressed in percentages (rB) as the median of the differences normalized by the Fi value and multiplied by 100:

$$B = Med\left\{y_{TQ,i} - y_{FI,i}\right\}, \text{and } rB = Med\left\{100 \bullet \frac{y_{TQ,i} - y_{FI,i}}{y_{FI,i}}\right\}$$

where Med is the median operator over a set of elements enclosed with the curly brackets. The significance of bias was tested using the nonparametric two-sided paired Wilcoxon Signed-Rank test at the 5% significance level. The null hypothesis was that there is no significant

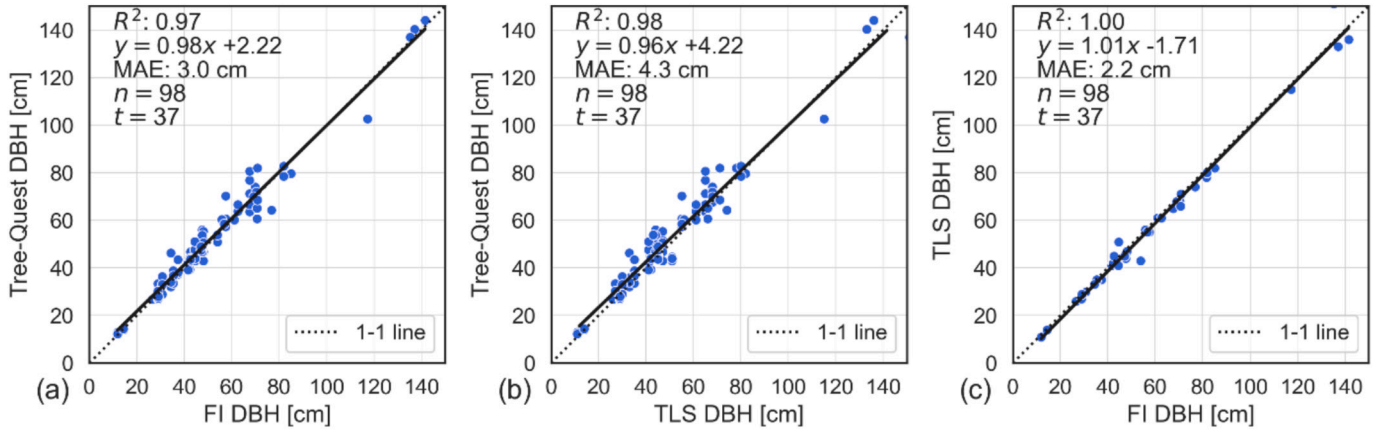

Fig. 6. High-quality single-tree DBH (diameter at breast height) measurements ($n = 98$) taken with Tree-Quest in Laxenburg Park, compared with (a) forest inventory (FI) DBH measurements, i.e., using DBH tape, (b) DBH measurements obtained with TLS; (c) Comparison between TLS and FI measurements of DBH. MAE is the mean absolute error, and R^2 is the marginal coefficient of determination. The number of trees with more than one measurement is $t = 37$, which is also the number of groups in the linear mixed model.

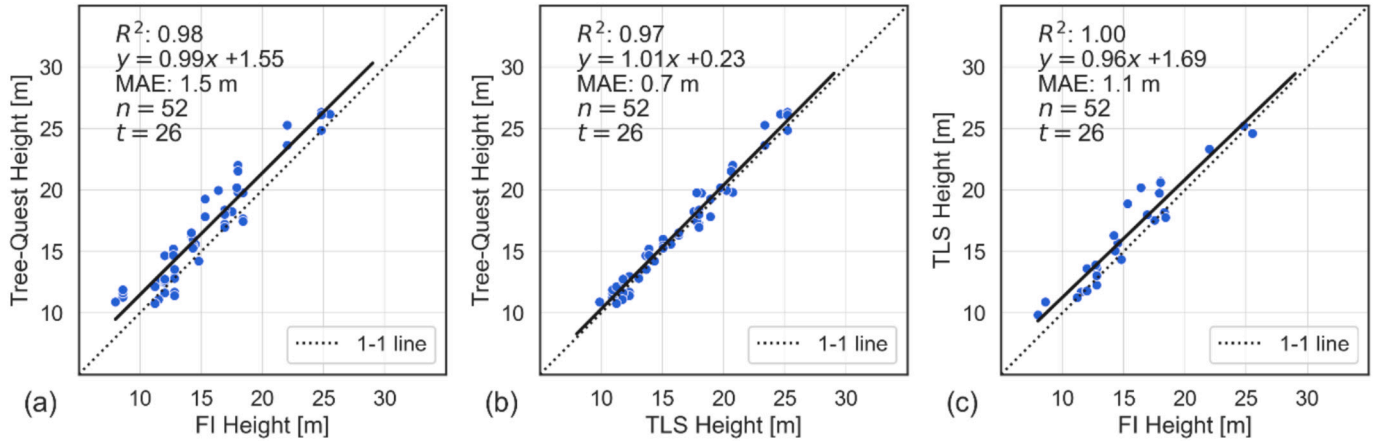

Fig. 7. High-quality single-tree TH (tree height) measurements ($n = 52$) taken with Tree-Quest in Laxenburg Park, compared with (a) forest inventory (FI) TH measurements, i.e., using laser range finder, (b) TH measurements with TLS; (c) Comparison between TLS and FI measurements of TH. MAE is the mean absolute error, and R^2 is the marginal coefficient of determination. The number of trees with more than one measurement is $t = 26$, which is also the number of groups in the linear mixed model.

bias between the paired observations. If the *p*-value is smaller than the significance level, the null hypothesis is rejected, and the bias is considered significant. The non-parametric test was used because the measurements did not meet the normality criterion, as indicated by the Q-Q plots and Shapiro-Wilk tests that we performed.

The measurements from different TQ groups are also tested to determine whether they are statistically interchangeable. Those groups include: (a) high-, medium-, or low-quality measurements, and (b) expert, practitioner, or student measurements. As these measurements belong to three groups, none of which met the normality condition, we used the nonparametric Friedman Test with the same significance level (0.05) as before. The imbalance in the number of measurements was addressed by randomly selecting subsamples from other groups to match the smallest group's sample size. The statistical interchangeability between DBH measurements acquired with the automatic and manual methods was tested as above using the Wilcoxon Signed-Rank test.

4. Results

4.1. Accuracy of the tree-quest measurements

The high-quality TQ DBH measurements were highly correlated with both the FI and TLS DBH measurements and associated with an MAE of 3.0 cm (rMAE 6.0%; RMSE 4.4 cm) and 4.3 cm (rMAE 9.1%; RMSE 5.6 cm), respectively (Fig. 6a and Fig. 6b). The corresponding regression lines show that the TQ measurements slightly overestimate the TLS measurements for DBH < 30 cm. For comparison, the TLS DBH correlates more closely with FI DBH and has a smaller MAE of 2.2 cm (rMAE 4.4%; RMSE 3.2 cm) compared to the TQ DBH. The results also showed that TQ measurements have a positive bias (overestimation) of 0.9 cm (1.6%) for FI measurements and 2.4 cm (5.0%) for TLS measurements. The TLS, however, showed a negative bias (underestimation) of −1.4 cm (2.6%) compared to FI measurements. All the biases were statistically significant according to their *p*-values from the Wilcoxon signed-rank test. The interclass correlation coefficient (ICC) was 0.07 in the TQ-FI DBH mixed model, indicating that 93% of the variance is due to measurement noise.

The TH measurements from TQ and TLS were more similar, with MAEs of 1.5 m (rMAE 10.7%; RMSE 1.8 m) and 1.1 m (rMAE 7.9%; RMSE 1.5 m), respectively, and with a high correlation ($R^2 > 0.97$) between one another (Fig. 7). As can be seen from their regression lines, both TQ and TLS heights overestimate the FI heights across the entire range of their values. The TQ heights had a bias of 1.1 m (7.0%) compared to the FI heights and 0.4 m (2.3%) to the TLS measurements. The TLS measurements also had a bias of 0.7 m (5.2%) to the FI measurements. All the biases were statistically significant. ICC was 0.67 in the TQ-FI TH mixed model, indicating that the between-tree variance dominated the measurement noise.

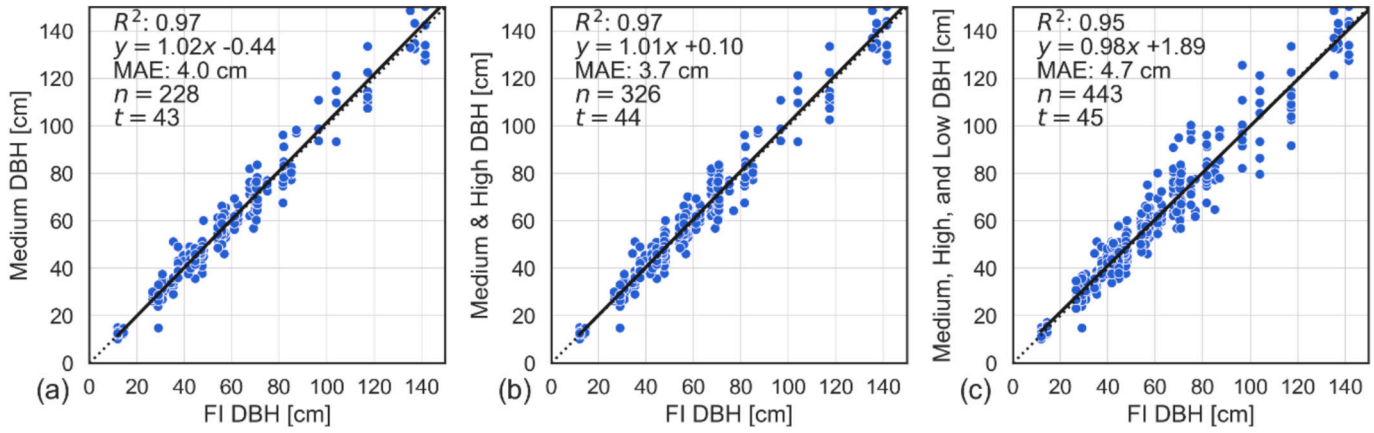

Fig. 8. The comparison of the Tree-Quest DBH (a) medium-quality measurements, (b) the combination of medium- and high-quality measurements, and (c) the combination of all three quality categories with the field inventory DBH measurements. t shows the number of unique trees with multiple measurements, which is also the number of groups in the linear mixed model.

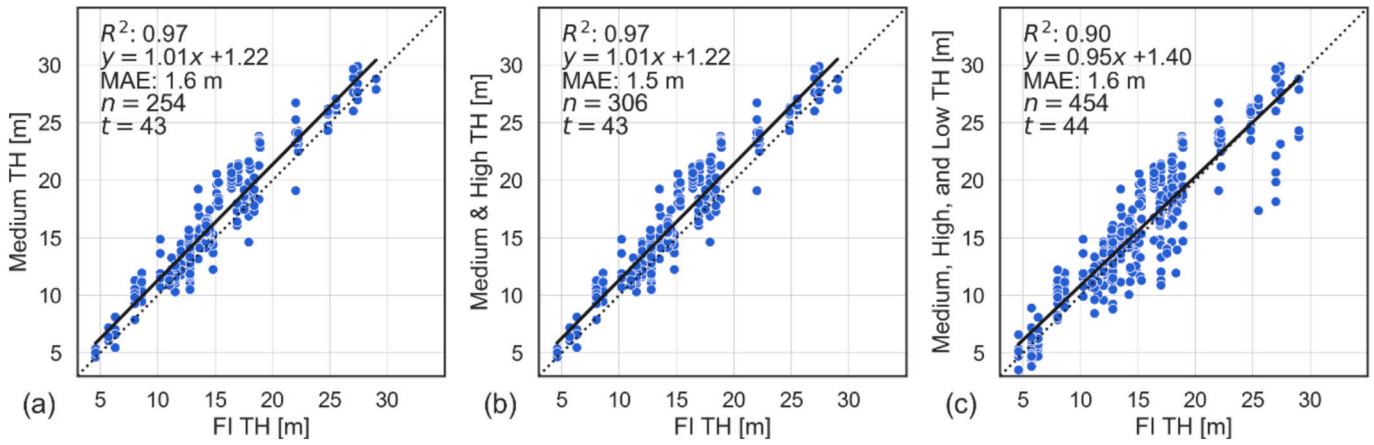

Fig. 9. The comparison of the Tree-Quest tree height (TH) (a) medium-quality measurements, (b) the combination of medium- and high-quality measurements, and (c) the combination of all three quality categories with the field inventory TH measurements. t shows the number of unique trees with multiple measurements, which is also the number of groups in the linear mixed model.

4.2. Quality categories and accuracy

To address the diverse measurement quality provided by different volunteers, TQ measurements were classified into high, medium, and low quality categories based on visual inspection of the app photos containing the AR objects – an AR circle for DBH measurement, and an AR cylinder for TH measurement (Section 3.4). The accuracy of the high-quality measurements is presented in Section 4.1, and here, we additionally present the accuracies of the medium-quality measurements, the combination of high- and medium-quality measurements, and the combination of all quality categories (low, medium, and high).

For DBH, the medium-quality measurements have an MAE of 4 cm (rMAE of 7.1%) (Fig. 8a), which is 1 cm higher compared to the MAE of the high-quality measurements (Fig. 6a). The combination of high- and medium-quality DBH measurements yields a slightly smaller MAE of 3.7 cm (rMAE 6.8%) than the medium-quality measurements alone. When measurements from all three categories are considered, the MAE increases to 4.7 cm (rMAE 8.0%), whereas the scatterplot shows that the dispersion of measurements also increases with an increase in the DBH (Fig. 8c) The biases of all three datasets were below 0.5 cm (~1%) compared to FI measurements. However, the bias in medium-quality measurements was not statistically significant (p-value = 0.49). In contrast, the biases in the other two datasets were found to be statistically significant, though with p-values close to the significance level (0.04 and 0.02). The Friedman test for the high, medium, and low DBH measurement groups indicated no statistical significance (p-value = 0.08). ICCs for the Medium, Medium & High, and all DBH quality measurements are 0.01, 0.07, and 0.19, respectively, suggesting measurement noise to be dominating source of variance.

For TH, the medium-quality measurements have an MAE of 1.6 m (rMAE 11.1%) (Fig. 9a), which is slightly higher than the MAE of the high-quality measurements (Fig. 7a). However, the combination of these two groups produces the same MAE as the high-quality measurements (Fig. 9b). Finally, the inclusion of the low-quality measurements with the other two categories resulted in a similar MAE, but the dispersion of points is larger, which decreased the R^2 (Fig. 9c). The biases of all three datasets to the FI measurements were found to be significant. The medium TH and medium & high TH measurements had 1.1 m (7.5%) bias, whereas the combination of all quality measurements had a bias of 0.6 m (5.1%). The Friedman test for the high, medium, and low TH measurement groups indicated no statistical significance (p-value = 0.22).ICCs for the Medium, Medium & High, and all TH quality measurements are 0.53, 0.56, and 0.27, respectively, indicating that MAEs of those groups were moderately affected by the variability within the tree and not purely on the measurement noise.

4.3. User groups and measurement quality

As discussed in Section 3.4, the volunteers were split, according to their familiarity with the app, into three citizen groups: experts, practitioners, and students. The DBH measurements by the expert and student user groups have a similar MAE that is just above 4 cm, but the

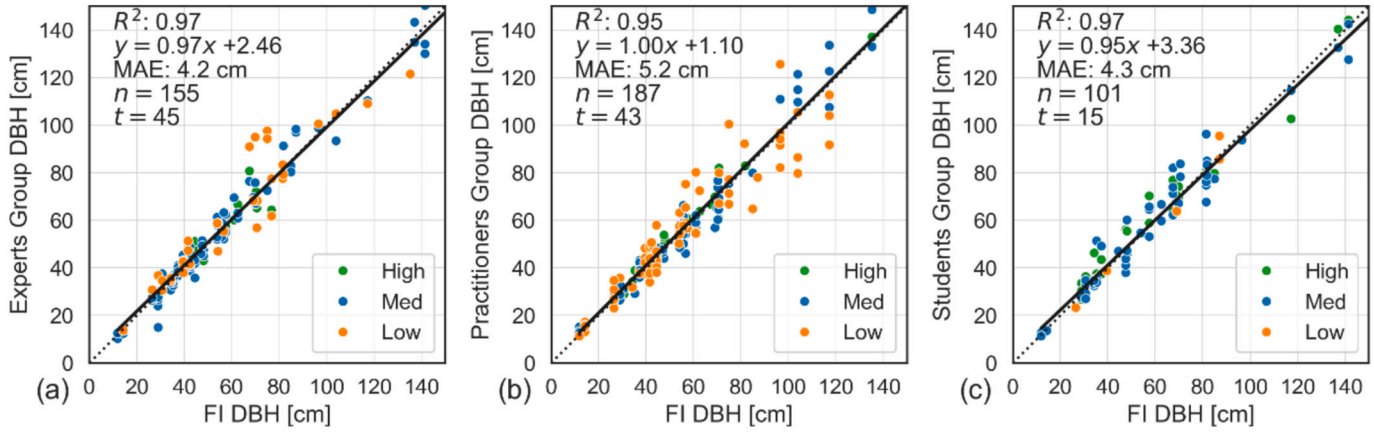

Fig. 10. The comparison of the Tree-Quest high, medium, and low DBH measurements acquired by (a) the Experts group, (b) the Practitioners group, and (c) the Students group with the field inventory DBH measurements. The points are colored according to their quality category. t shows the number of groups in the linear mixed model.

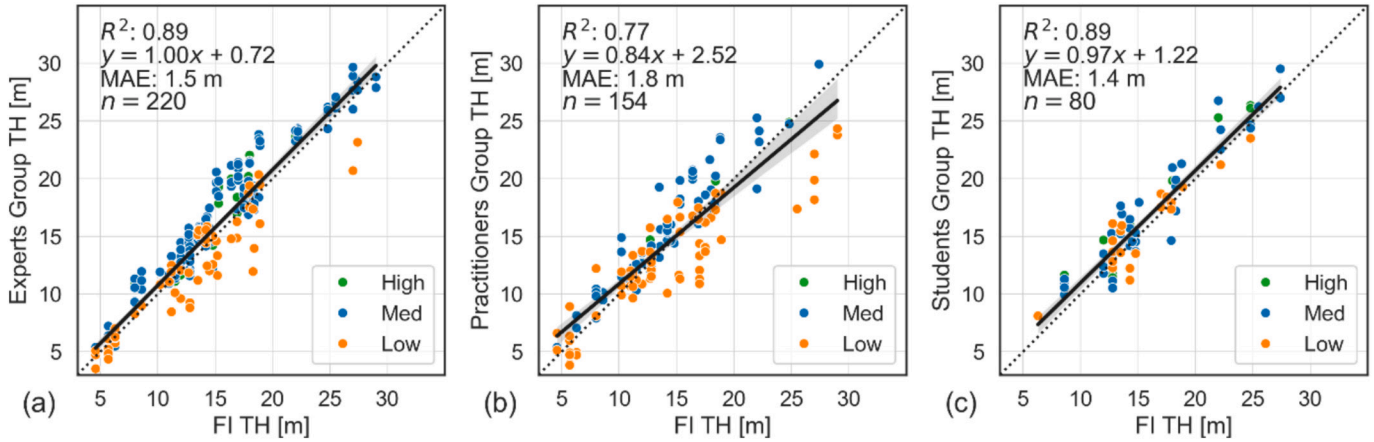

Fig. 11. The comparison of the Tree-Quest high, medium, and low TH measurements acquired by (a) the expert group, (b) the practitioner group, and (c) the student group with the field inventory DBH measurements. The points are colored according to their quality group.

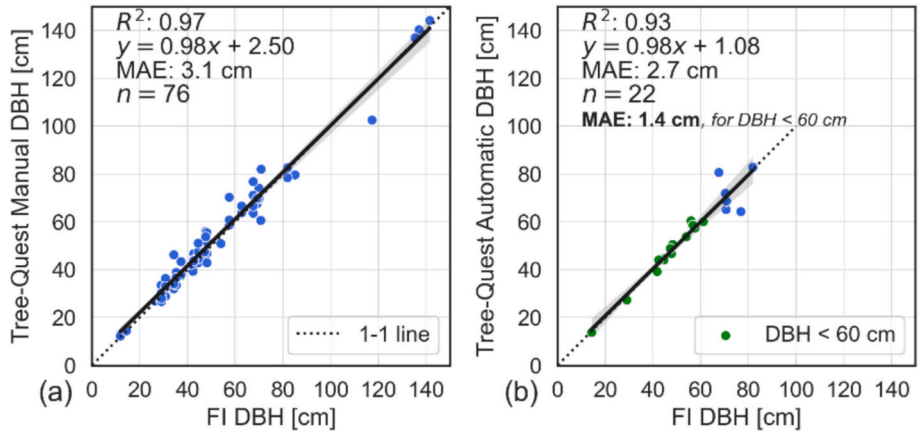

Fig. 12. High-quality DBH measurements from Laxenburg Park acquired using two different Tee-Quest DBH measurement methods: (a) the manual, i.e., angular, approach, (b) the automatic, i.e., circle fit, approach.

student group contained just a few low-quality points (Fig. 10a and Fig. 10c). The practitioner group had the largest MAE of 5.2 cm and also many low-quality points (Fig. 10b). The biases in student and expert groups compared to the FI measurements were not significant (*p*-values of 0.60 and 0.34, respectively). The bias in practitioner data was 0.7 cm (1.6%) and was shown to be significant. The Friedman test for the expert, practitioner, and student DBH measurements indicated no statistical significance (p-value = 0.09). Low-to-moderate mixed effects for each user were observed only in the Student group (ICC = 0.11), whereas the other groups' ICCs were below 0.015. The moderate mixed effects for each tree were observed only in the Expert group (ICC = 0.28), whereas the Students and Practitioners groups had ICCs below 0.02. This means that MAE for the Student and Practitioner group was driven by the measurement noise, whereas MAE of the Expert group was a pessimistic estimate as moderately impacted by within-tree variability.

For the TH measurements, all three user groups had an MAE between 1.4 and 1.8 m (Fig. 11), which is also in the range of the MAE values from different data quality groups (Fig. 7 and Fig. 9). The expert and student groups had the largest R^2, and their regression models show a small but consistent underestimation along all TH values. The regression model for the practitioner group, in contrast, showed underestimation of small TH (i.e., <15 m) and overestimation of high TH values (i.e., >20 m). In addition, the majority of low-quality measurements in the expert and practitioner groups underestimated the TH. The biases of 0.7 m (5.5%), 0.6 m (4.9%), and 0.7 m (3.9%) in expert, practitioner, and student TH measurements, respectively, compared to FI measurements were significant. The Friedman test for the expert, practitioner, and student DBH measurements was statistically significant (p-value = 0.02).

4.4. Automatic and manual DBH measurement methods

Among the high-quality DBH measurements, 78% were acquired using the manual, i.e., angular, DBH method, whereas only 22% were acquired using the automatic, i.e., circle fit, method. The MAEs for manual and automatic DBH measurements were 3.1 cm and 2.7 cm, respectively (Fig. 12), similar to the one reported for all data (Fig. 6a). However, the automatic DBH measurements were more accurate for the trees with a DBH below 60 cm, with an MAE of 1.4 cm (rMAE 3.3%; RMSE 1.8 cm). The regression lines of both methods show almost no bias, with the manual method overestimating small DBH values slightly more than the automatic method. A statistically significant bias (p-value 0.001) of 1.1 cm (1.9%) was observed in manually measured DBH values compared with those obtained with the FI method. However, for automatic DBH measurements, no significant bias was observed (p-value 0.80). Only 15 trees shared paired manual and automatic high-quality DBH measurements, showing a statistically significant bias of −1.8 cm (2.3%, p-value 0.40)

4.5. Comparison with other apps

The TQ DBH measurements had the smallest MAE compared to those acquired with the other two apps in the Stadtpark test site (Fig. 13). Nevertheless, the MAE of the TQ and GreenLens apps were comparable, whereas the Working Trees app's MAE was almost twice as large. Furthermore, the regression line for the TQ DBH measurements showed almost no bias, i.e., the slope of the model was 1, but the intercept indicates a mm-scale overestimation (< 0.5%). Furthermore, the MAE of the TQ measurements was comparable to the MAE of the high-quality TQ measurements in Laxenburg Park (Fig. 6a). The DBH measurements acquired by the GreenLens app were overestimated, whereas the Working Trees measurements mostly underestimated the FI DBH values. However, the biases in TQ, GreenLens, and Working Trees DBH measurements (0.2 cm, 0.4 cm, and 1.1 cm) relative to the FI measurements were not significant (*p*-values of 1.00, 0.90, and 0.49, respectively).

The TQ TH measurements had the smallest MAE again compared to those acquired with the other two apps in Stadtpark (Fig. 14). The TQ MAE was comparable to the MAE of the high-quality TQ measurements in Laxenburg Park (Fig. 7a). Nevertheless, the regression models showed that all three apps acquired heights that consistently overestimated the FI TH values. The biases of 0.7 m (5.0%), 1.0 m (7.8%), and 0.7 m (5.0%) in TQ, GreenLens, and Working Trees TH measurements relative to the FI measurements were found significant (p-values of 0.021, 0.004, and 0.016).

5. Discussion

5.1. Tree-quest measurements

The analysis showed that the accuracy of TQ DBH measurements was more sensitive than the accuracy of the TQ TH measurements when low-quality measurements were added. The MAE of DBH ranged from 3 cm (rMAE 6%) for high-quality measurements to 4.7 cm (rMAE 8%) when the medium– and low-quality measurements were added. The MAE also increased to 5.2 cm (rMAE 8.6%) for the measurements from the practitioner group. For TH, the MAE ranged from 1.3 to 1.5 m (rMAE 8.7–11%) for different test sites, measurement qualities, and user groups. Only the practitioner group measurements resulted in a higher MAE of 1.8 m. These results show that data curation has an impact on the MAE of both DBH and TH measurements. The results also show that different citizen groups have an impact on the MAE of both DBH and TH measurements. However, it should be noted that the number of

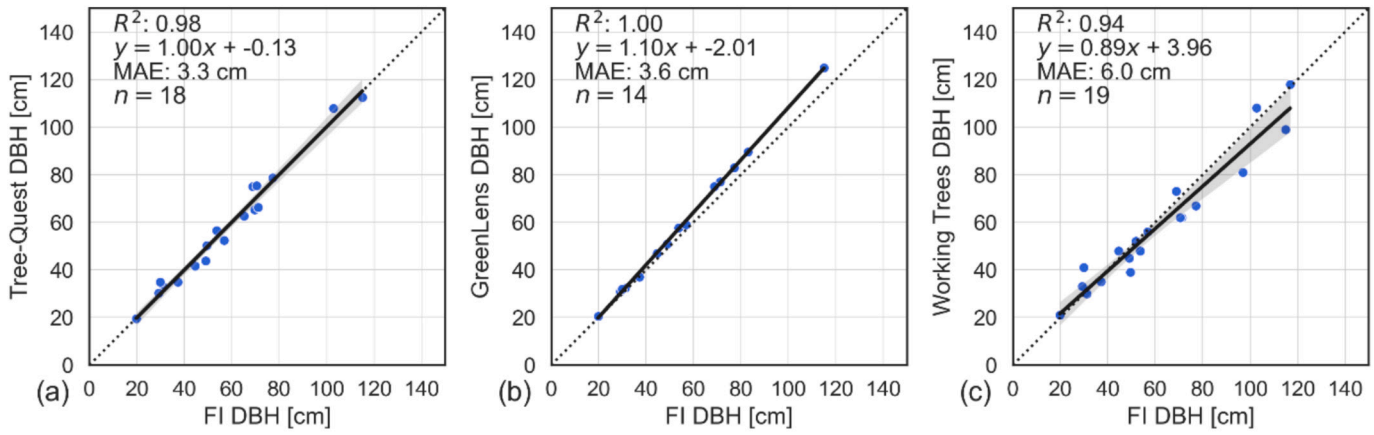

Fig. 13. Comparison of the DBH measurements acquired with (a) the Tree-Quest app, (b) the GreenLens app, and (c) the Working Trees app with the field inventory (FI), i.e., tape measurements for the trees in Stadtpark.

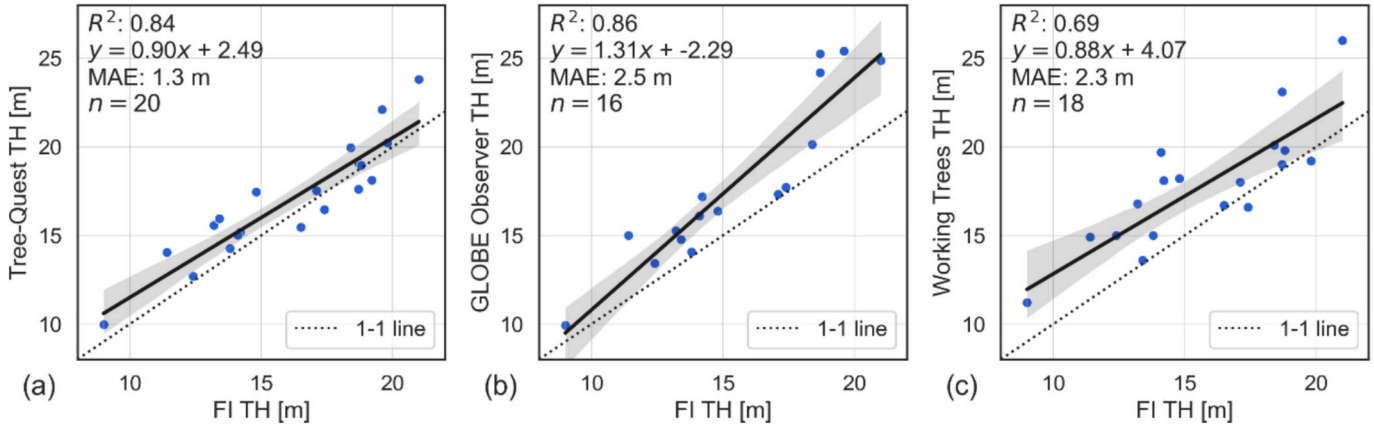

Fig. 14. Comparison of tree height (TH) measurements acquired with (a) the Tree-Quest app, (b) the GLOBE Observer app, and (c) the Working Trees app with the field inventory (FI) measurements for the trees in Stadtpark.

measurements in those groups was not controlled, so that sample size imbalance may also affect the resulting MAE.

The bias analysis of DBH measurements showed that all citizen groups and quality groups had small biases ($\leq$ 2%) relative to the FI measurements. The overestimation of high-quality DBH measurements of 0.9 cm (1.6%) was statistically significant. This implies that TQ and FI data can be used jointly only after removing the bias between them, for example, by applying a mixed model that accounts for it. The statistical analysis of manual and automatic DBH measurements revealed that manual DBH measurements drive the above bias, as the bias between automatic and FI DBH measurements was not statistically significant. The analysis further showed that TQ, FI, and TLS DBH measurements were also statistically different, so they can be used jointly only after removing the biases between them, e.g., when applying a mixed model with groups corresponding to data source (e.g., TQ, TLS, and FI) to account for biases due to their measurement errors. The Friedman test, however, showed that groups with high-, medium-, and low-quality DBH measurements were not statistically different, indicating that they introduced the same bias to the FI measurements. The same was shown also for the experts, practitioners, and student groups.

The biases in TH measurements from citizen groups and quality groups were all statistically significant, introducing 3.9% to 7.8% overestimation of the FI measurements. The Friedman test showed that TH measurements across those groups were statistically different, indicating that they lead to different biases compared to FI or TLS measurements of TH. The overestimation of high-quality TH measurements was 1.1 m (7%), but TLS measurements also overestimated FI measurements by 0.7 m (5.2%). The latter overestimation is surprising, given that laser scanning from the ground, due to canopy elements, is expected to underestimate tree height (Liang et al., 2018). Our TLS, however, was conducted on detached trees with minimal crown overlap, a setting expected to capture crown-top returns accurately without producing erroneous returns above the canopy. Therefore, this overestimation might instead indicate that our FI measurements underestimated real tree height.

To understand the impact of measurement errors in TQ DBH and TH on aboveground biomass (AGB), we used several allometric equations to propagate these errors into the AGB estimates. This was done using species-specific allometric equations for total AGB (Muukkonen and Mäkipää, 2006; Zianis et al., 2005), which were available only for three species in our study. For each of those species, we additionally used the allometric equation from (Chave et al., 2014) that is commonly used particularly popular in remote sensing AGB studies. The propagation of the DBH and TH errors from the high-quality TQ measurements (MAE of 6%, and 11%, respectively) resulted in an AGB estimate error ranging from 6% to 20%, depending on the tree species and the allometric equation used. Those results are summarized in Table B. 1, Appendix B. The above uncertainty is aton a tree level, and estimates aton the plot level would, due to averaging over n trees, lead to a reduced uncertainty with a factor of $\sqrt{n}$. Just averaging over 16 trees would reduce the highest AGB estimate uncertainty in Table B. 1 to under 5% of the AGB estimate. Therefore, although TQ DBH and TH measurements may introduce uncertainties up to 20% at the single tree level, they can be particularly useful for plot-level AGB estimates, for example, as a

ground reference for calibration of satellite images, as their pixels commonly include several trees. This error propagation also confirmed findings from other studies that the selection of the allometric equation and sampling design are the dominant sources of error in plot-level AGB estimates. As the inclusion of low-quality TQ measurements increases DBH uncertainty, the propagation of such TQ measurements would result in larger AGB errors compared to those in Table B. 1, which again shows the importance of data quality curation before further utilization.

The above discussion assumes that tree species identification is error-free, which does not hold in crowdsourced species recognition and may affect AGB estimates through the selection of species-specific allometric equations and wood density. We did not evaluate the Pl@ntNet API independently in this study, but its performance has been assessed in several recent studies. Overall, these studies show that Pl@ntNet and comparable AI-based plant-identification tools can provide high identification accuracy, particularly for common, well-documented taxa and when several informative plant images are available, but that accuracy remains context-, taxon-, image-, and organ-dependent. Hart et al. (2023) reported that Pl@ntNet correctly identified plants as its first choice in about 87% of cases, whereas the correct taxon was included among the top five suggestions in about 95% of cases. In a study that included 55 urban tree species, Pl@ntNet correctly identified approximately 71% of species and 88% of genera; species-level accuracy increased to nearly 87% when leaf images were used, but decreased to about 55% when only bark images were used (Schmidt et al., 2022). This organ dependence is consistent with the broader evaluation of automated plant-identification tools in Switzerland by Popp et al. (2025), who showed that identification success improves when multiple images and multiple plant organs are supplied, with up to 85% of species observations correctly identified across automated services, while images of bark and vegetative graminoids were more challenging. Popp et al. (2025) also showed, in an evaluation of 5000 photos of 564 vascular plant species, that global services such as Pl@ntNet and iNaturalist offer broad taxonomic coverage, whereas regionally tailored systems may achieve higher accuracy when their geographic scope and taxonomic concepts match the study region. More generally, Renner (2026) emphasized that AI-based plant-identification tools are becoming essential components of modern floristic workflows, but also noted that they should be linked to curated images, taxonomic expertise, and dynamic quality-control processes rather than treated as infallible replacements for expert identification. Similarly, Enríquez-de-Salamanca (2025) highlighted that botanical databases and citizen-science records are valuable for biodiversity assessments but require careful validation because AI-assisted identifications may be less reliable for rare, endemic, threatened, or diagnostically difficult taxa, especially when conventional photographs do not capture the relevant morphological characters. Recent work on Pl@ntNet's cooperative learning framework further shows that the platform addresses these limitations through human–AI interaction, estimating user expertise and filtering unreliable observations; this strategy improved label recovery compared with simple majority-vote approaches, especially in ambiguous cases (Lefort et al., 2026). Lefort et al. (2026) also showed that integrating AI predictions with human votes can further improve post-processing, provided that AI confidence is calibrated and model collapse is avoided. Finally, Bonnet et al. (2025) stressed that citizen-generated AI-assisted plant observations can support biodiversity monitoring only when calibrated uncertainty and transparent metadata are preserved. Thus, while the integrated Pl@ntNet API substantially simplifies the Tree-Quest workflow and provides a useful first step for species identification, incorrect species assignment remains a potential additional source of uncertainty in downstream AGB estimation. Therefore, for applications requiring high confidence, especially for rare or taxonomically difficult trees, we recommend that Tree-Quest species identifications be supported by multiple organ photographs, and, where possible, expert or community validation before the data are used in AGB estimation.

The results also showed that TQ DBH measurements were comparable to those of other apps. The biases of each app's measurements to FI measurements were found not statistically significant. The TQ MAE was the smallest among the three apps for the Stadtpark measurements (Fig. 13). Interestingly, those MAEs were almost twice as large as the MAE and the mean error reported in the original studies of the two apps (Ahamed et al., 2023; Feng et al., 2024). One explanation is that the original studies considered only trees with a DBH below 60 cm, and our study included many larger trees (up to 116.9 cm in Stadtpark and 160 cm in Laxenburg Park), that are more challenging to measure. When we considered only trees with a DBH below 60 cm in Laxenburg Park that were measured with the automatic circle fit method (Fig. 12b), our MAE was also reduced by more than half, to 1.4 cm. Although our sample for this MAE was small (only 17 measurements), it still indicates that including larger trees in the analysis may lead to higher MAE. This is because large trees are more difficult to measure because of their irregular stem shape and the side from which they are measured. Yet, TQ DBH measurements are as good as those from other apps. As with DBH, TQ TH measurements had the smallest MAE and, thus, were comparable to the other two apps. However, the biases in TH measurements from each app relative to FI measurements were all statistically significant, ranging from 0.7 m to 1.0 m. Thus, those biases shall be considered in the further use of TH measurements and in uncertainty estimation when propagated, e.g., in aboveground biomass estimation. Determining which app is the most accurate was beyond the scope of this study and would require a different experimental design. Compared with TLS, TQ DBH and TH measurements had a higher rMAE by 1.6% and 2.8%, respectively. Nevertheless, while TQ offers direct and free measurements, TLS involves expensive equipment and data processing that can be advantageous when a comprehensive forest plot assessment is necessary, i.e., beyond TH and DBH information.

Finally, FI measurements in our study were collected by a single experienced operator and were not replicated by multiple observers. Therefore, we cannot directly quantify inter-observer variability from our dataset. However, previous studies have shown that conventional field measurements of DBH are generally highly repeatable. For example, when four trained specialists independently measured 319 trees, the standard deviation of DBH measurements was only 0.3 cm, corresponding to approximately 1.5% of the measured value, and no statistically significant differences among observers were detected (Luoma et al., 2017). In contrast, tree height (TH) measurements exhibited greater variability, with a standard deviation of 0.5 m (2.9%) among observers. These findings suggest that DBH measurements obtained by trained personnel are typically associated with uncertainties on the order of 1–3%, whereas TH measurements generally exhibit somewhat larger uncertainty.

5.2. *Advantages*

The existing apps for single tree measurements are, like Tree-Quest, freely available, can work offline, and provide comparably accurate measurements. Tree-Quest has, however, several additional characteristics that are more tailored for citizen-science ground data collection. Our app features a modular structure and can be customized by initiating specific quests tailored to the needs of different user groups, such as scientific experts, forest owners, and citizens. Then, the app's measurements are made available to citizens through an open data portal that also features a leaderboard and supports citizen engagement through gamification. Also, TQ collects AR images during measurements, enabling high-quality data curation before further application.

The TQ's modular design allows for customization to meet specific goals. For example, besides an opportunistic quest, where the user can select any tree to measure, TQ also supports guided quests that direct participants to survey specific, pre-selected trees. The data for this study were acquired from two such quests, one from Laxenburg Park and one from Stadtpark trees. These guided quests included all the TQ modules

(DBH, TH, tree species identification, and questionnaire). Still, they were limited only to the predefined trees marked on the app's base map, helping users to identify the trees easily. However, it is possible to design other quests, e.g., that include only DBH and exclude TH, tree species identification, and the questionnaire. The app also features an expert mode, accessible through the main settings, which allows for the fine-tuning of some AR parameters and the disabling of certain modules (Fig. 2h). This can be particularly handy when the measurement time needs to be reduced, e.g., for an efficient expert survey of a forest plot or a citizen campaign focused on one or a few variables.

The advantage of the guided quest is that often, there is ground truth data for all or some of the trees. The reference data can then be used to control the measurement quality and engage with citizens through gamification. In the Laxenburg Park quest, e.g., we used the reference data to score each measurement of the student group and awarded the three students with the highest score (Fig. A.1 in Appendix A **Error! Reference source not found.**). This may be one of the reasons why the student group outperformed the practitioner group in DBH and TH measurements (Section 4.3). Gamification can also be implemented without reference measurements, e.g., by considering the number of provided measurements or the overall measurement quality, as the latter can be derived from the screenshots with AR objects.

The TQ advantage is also that it collects auxiliary images with AR objects, allowing for the assessment of the quality of the citizen data in postprocessing. Fig. A.2 (Appendix A). Shows examples of high- and low-quality DBH and TH measurements from Laxenburg Park. That quality information is particularly important for citizen science campaigns, where the quality of the acquired citizen measurements is expected to be highly diverse. Thus, the possibility of labeling citizen measurements into different quality categories provides more homogeneous data and more control in the subsequent application of the data, such as biomass and carbon mapping.

Another TQ advantage is that it can also work offline. The base map can be downloaded before going to the field when the internet is available. The photo upload for Pl@ntNet identification and uploading completed quests can be done after returning from the field, when the internet is available again. This is particularly relevant for measuring single trees in areas with poor mobile internet coverage, such as remote areas or developing countries. Therefore, our app is flexible in design, can introduce new opportunistic or guided quests, and supports gamification, which provides a solid framework for collecting citizen-science-based measurements for biomass and carbon mapping of trees in natural or urban settings.

5.3. Limitations and recommendations

The analysis showed that many low-quality DBH measurements were associated with trees of large diameter. In the measurements from the expert and practitioner groups (Fig. 10a Fig. 10b), low-quality points were more scattered away from the model than other measurements, particularly for DBH $>$ 60 cm. The same pattern could be seen when low-quality measurements were added to the high- and medium-quality sets (Fig. 8b and 6c). Measuring large DBHs with the automatic method was also challenging from our experience, as we observed that the automatic circle fit method often picks up feature points from the basal shoots, small bushes, or tall grass around the trees, leading to an erroneous DBH measurement (Fig. A.2a in Appendix A). This shows that trees with large DBH are more challenging to measure, and a user may expect some low-quality TQ measurements in such cases. Measurements with the manual DBH method, however, worked without problems on large trees.

To maximize DBH accuracy, we recommend the automatic (circle fit) method only for measuring trees with DBH $<$ 60 cm (Fig. 12b) and with little or no understory. For trees with a DBH $>$ 60 cm, or where understory is present, we recommend using the manual DBH method. This method is superior in the case of understory as it does not rely on automatic selection of feature points but rather on how well the user aligns the vertical AR line with the trunk sides (Figure A.2b). Furthermore, we recommend additional data quality curation to remove low-quality measurements, which resulted in an MAE of less than 4 cm (rMAE $<$7%).

More practical recommendations include that the user moves at least one quarter around the tree to obtain more complete feature points of the trunk and improve the circle fit. If the circle gets erroneously large, we recommend selecting the Back button and repeating the measurement. In the Laxenburg campaign, we recommended repeating this process a maximum of three times and retaining the last erroneous measurement if the fit does not improve, for use in the post-processing data curation step. The user should also consider the sun's location before taking measurements. The sun can cast direct light on the scene, reducing the visibility of feature points and the base map. Low visibility of the base map may also lead to inaccurate tree location during the user selection on the map. Also, because we rely on a phone camera, a passive sensor, the app can perform measurements only when (sun-) light is available in the scene. Relying only on the phone's GNSS location may also be inaccurate, particularly in dense stand (Tomaštík Jr. et al., 2017). Thus, it is recommended to measure several neighboring trees and use area averages for more accurate mapping.

In our study, we observed that low-quality TH measurements were almost systematically clustered below other points, resulting in an underestimation of TH (Fig. 11). We discussed this with the practitioner group and realized there was a misinterpretation of the TH definition before the campaign. The app renders an AR cylinder, and they assumed that the cylinder volume is to compensate for the whole tree volume, and thus, they systematically introduced measurements below the top of the tree. This shows the importance of clearly communicating and defining each measurement in a citizen science campaign. In addition, reduced visibility of the treetop due to occlusion by its wide crown, neighboring trees, or the sun can also result in low-quality TH measurements. To minimize this, we recommend selecting the tree side from which the treetop is best visible, stepping back at approximately the same distance as the tree height, and finally collecting the treetop measurement. A dense forest with overlapping tree crowns would be a particularly challenging environment because of the limited visibility of the treetops. Finally, TH measurement quality depends on how accurately a user points at the top and bottom of a tree (**Error! Reference source not found.**c and **Error! Reference source not found.**d), but looking at the AR screenshots, TH measurements can be quality curated.

It is noted that our test site conditions were more typical for trees outside forests. They included rather sparse trees, planted on flat park areas, offering good tree-top visibility and light conditions, and free space to walk around the trees. Those conditions in a real forest can be more challenging, which may impact the app's performance. Nevertheless, this study shows that the app and citizen-science approach can effectively measure trees outside forests, which can potentially complement the NFI data of trees in forests. A comparison of the app measurements with NFI data was beyond the scope of this paper, but that would be an important and necessary step to understand how to best combine these two sources of information in assessing the carbon stored in trees.

The potential application of TQ in forests would require additional testing on forest plots with different, e.g., stand types, canopy densities, slopes, and understories, to understand how TQ performs across diverse forest stand conditions. An additional way forward is to assess how TQ measurements can complement airborne LiDAR data for operational tree-level forest planning (Pascual, 2021; Vauhkonen, 2020). Another application could be the calibration and validation of forest products derived from satellite data, e.g., global canopy height models derived from satellite LiDAR (Pascual et al., 2022) or tree height and above-ground biomass density products from the novel ESA P-band radar BIOMASS satellite (Banda et al., 2025a; Banda et al., 2025b). In this way, TQ would also have to be extended beyond single-tree measurements to an area-based assessment of forest structure. Measurement

time for a full single-tree survey using our app can often be long and require considerable effort, especially for beginners. This is mostly because the survey includes several modules (DBH, TH, species recognition, and questionnaire), but also due to the interaction with AR objects that citizens need time to master. This affects citizen engagement, as observed by the student group, where 40% of volunteers gave up after surveying one or two trees, while the remaining volunteers surveyed about 10 trees on average. Volunteers who were more familiar with forestry (practitioners and experts) also provided more measurements and showed an appreciation of the variability of available tools. Thus, our app would need more simplification to be better suited for non-experts and increase citizen engagement. One possible improvement for that can be the automation of stem recognition, e.g., similar to that in Feng et al. (2024), which can simplify app use and ensure consistent measurements, thereby reducing the measurement time and improving user engagement.

Different phone models can also affect TH and DBH measurement errors. Phones come with varying cameras, inertial measurement unit (accelerometers and gyroscopes) capabilities, potential integration of depth sensors (ToF or LiDAR), and different processing power. This affects the performance of the Visual-Internal SLAM (VISLAM) algorithm and, in turn, the accuracy of the resulting AR measurements (Philippsen et al., 2020). Some contemporary iOS and Android phones, such as the Google Pixel 5 and iPhone 16, offer higher processing power (8- or 6-core CPUs and 8 GB RAM) and support 60 frames per second with ARCore and ARKit. Other, mostly non-Google Android phones with lower processing power, are limited to 30 frames per second when running VISLAM, which may result in fewer feature points and higher localization and mapping errors (Nowacki and Woda, 2020). That study also showed that AR depth estimation may be affected by abrupt phone motion, as it can introduce motion blur and reduce the number of feature points. Furthermore, VISLAM assumes that the scene is static while the camera is in motion. Thus, AR may underperform when understory moves during a DBH measurement, e.g., due to wind. Furthermore, noise and the initialization of the inertial measurement unit may introduce scale drift in longer AR sessions. Those AR limitations may be more pronounced on older phones, where simplifications of VISLAM might be required to run smoothly on their limited processing power. Studying the impact of the above aspects on TH and DBH errors would require careful selection of representative phones and an appropriate sample size, which was beyond the scope of this study's experimental setup. Finally, other apps (beyond TQ, GreenLens, Working Trees, GLOBE explored in our experiments) and other systems collect citizen-based data on trees outside forests, without providing automated DBH, TH, or species identification. For example, iTree is a collection of web and mobile app tools that help assess the benefits of local trees and select a tree for planting, considering its potential benefits (Nowak, 2024). In contrast to TQ, iTree does not measure DBH or tree species, but rather asks the user to enter those values manually if known, so the benefits of that tree can be calculated. TreeSnap is another app focused on documenting tree occurrences, health symptoms, and genetic or pest-related traits, supplying researchers with large geo-tagged photo datasets (Crocker et al., 2020). In contrast to automatic tree species identification in TQ and Pl@ntNET, TreeSnap engages users by providing guidelines for tree species identification and asking them to enter DBH and TH values manually. Finally, OpenTreeMap is an open platform for crowdsourcing tree inventories that allows users to add and share trees individually and calculate their benefits (Azavea and Urban Ecos, 2025). The platform provides search, filtering, and editing capabilities to manually add or edit single-tree information, including DBH, TH, and species. These apparent complementarities with TQ offer a possibility for joint exploration in future citizen-based studies.

6. Conclusions

In this paper, we presented Tree-Quest, a free citizen-science mobile app for measuring single-tree attributes, including DBH, TH, and tree species identification. Based on our initial results, the tool provides a solid workflow for collecting citizen-science-based measurements of tree biomass and carbon-related storage of tree attributes mapping information for trees outside forests. However, we also learned some lessons about using the app. For example, the automatic (circle fit) method performs better for trees with DBH < 60 cm and without understory, while the manual DBH method is better suited to large trees or those with understory. Furthermore, we observed that the manual method introduced a statistically significant bias of $\sim$1 cm ($<$2%) to its DBH measurements, which was not the case for the automatic method. Data quality was also an issue, so data curation is important for filtering out low-quality measurements. The high-quality DBH and TH measurements yield the lowest MAEs of 3 cm (6%) and 1.5 m (11%), respectively. The app also introduced a statistically significant bias of 1.1 m (7%) in its TH measurements. Thus, the bias in DBH and TH measurements shall be accounted for before joint use of the TQ and FI data in, e.g., plot-level aboveground biomass estimation. The app stores screenshots of AR objects: an AR circle during DBH measurement, and an AR cylinder during the TH measurement, which can be used to determine the quality of the Tree-Quest measurements. As it is valuable for curating data from citizen science campaigns, we performed this step manually, but this feature will be automated in the future to support large-scale citizen science campaigns. Another possible improvement will be the automation of the DBH measurements. Finally, the testing here was primarily undertaken on trees outside of forests, soand therefore these results cannot be generalized to the measurement of trees in forests. In the future, we plan to test the app more extensively in forest areas as a tool that can also be used by experts.

Data and code availability

The data and code necessary to reproduce the results of this study have been made available in the following repositories: GitHub: https://github.com/MilutinMM/TreeQuestPaper.git. Zenodo: https://doi.org/10.5281/zenodo.18063770

CRediT authorship contribution statement

Milutin Milenković: Writing – review & editing, Writing – original draft, Visualization, Validation, Supervision, Project administration, Methodology, Investigation, Funding acquisition, Formal analysis, Data curation, Conceptualization. **Florian Hofhansl:** Writing – review & editing, Writing – original draft, Validation, Methodology, Formal analysis, Data curation. **Rudi Weinacker:** Writing – review & editing, Software, Data curation. **Tobias Sturn:** Writing – review & editing, Software, Data curation. **Santosh Karanam:** Writing – review & editing, Software, Data curation. **Benjamin Wild:** Writing – original draft, Methodology, Data curation. **Markus Hollaus:** Writing – review & editing, Methodology, Funding acquisition, Data curation. **Christoph Neumayr:** Writing – review & editing, Data curation. **Anna Iglseder:** Writing – review & editing, Data curation. **Norbert Pfeifer:** Writing – review & editing, Supervision, Funding acquisition. **Luca Zappa:** Writing – review & editing, Data curation. **Viktor J. Bruckman:** Writing – review & editing, Funding acquisition, Data curation. **Roman Breitfuss-Schiffer:** Writing – review & editing, Data curation. **Benjamin Schumacher:** Writing – review & editing, Funding acquisition. **Hugo Gresse:** Writing – review & editing, Software. **Alexis Joly:** Writing – review & editing, Software. **Pierre Bonnet:** Writing – review & editing, Software. **Dmitry Schepaschenko:** Writing – review & editing, Methodology, Data curation. **Linda See:** Writing – review & editing, Writing – original draft, Data curation. **Ian McCallum:** Writing – review & editing, Supervision, Data curation. **Steffen Fritz:** Writing – review & editing, Supervision, Funding acquisition, Conceptualization.

Declaration of competing interest

The authors declare that they have no known competing financial interests or personal relationships that could have appeared to influence the work reported in this paper.

Acknowledgments

The work was conducted within the C4C project, funded by the Austrian Research Promotion Agency (FFG) under the ASAP 2022 call (Application ID: 47907528), and the OEMC project, which received funding from the European Union's Horizon Europe research and innovation programme under grant agreement No. 101059548. We would also like to thank the Pl@ntNet team for their support during the integration of Pl@ntNet API in Tree-Quest's tree spaces module.

The authors gratefully acknowledge funding from IIASA and the National (and Regional) Member Organizations that support the institute.

Appendix A. Appendix

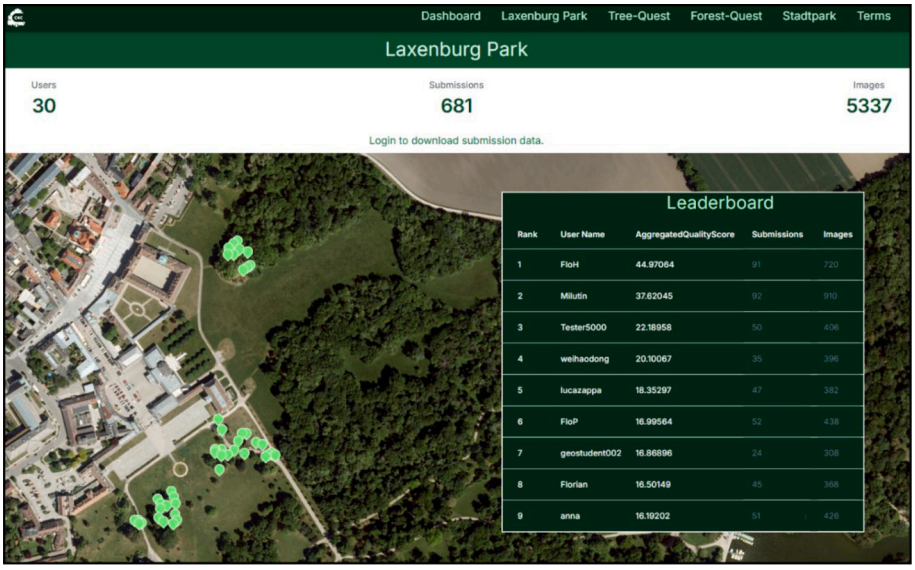

Fig. A.1. An example of the data portal for the Laxenburg Park Quest, a guided TQ quest, and the leaderboard with nine top-ranked volunteers and details about their submissions. The green pins show the predefined trees that citizens shall visit and measure. (www.c4cweb.main.geo-wiki.org). (For interpretation of the references to colour in this figure legend, the reader is referred to the web version of this article.)

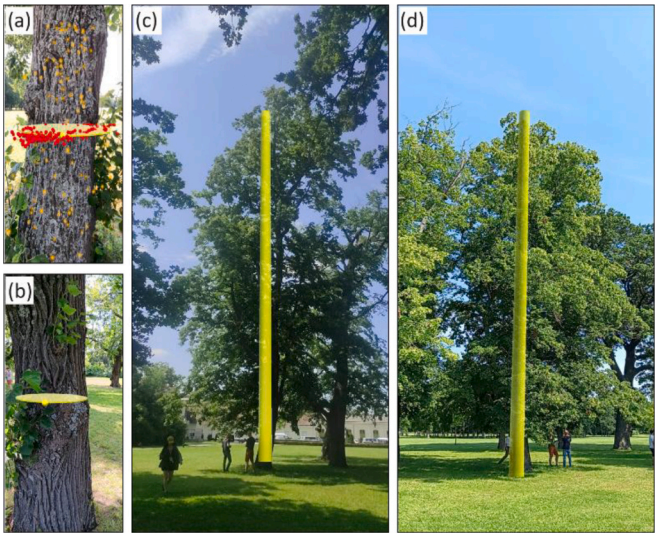

Fig. A.2. Screenshots taken by the app during DBH measurements of trees with basal shoots with (a) the automatic circle fit method leading to a low-quality measurement, and (b) the manual method leading to a high-quality DBH measurement. Screenshots were taken during (a) a low-quality and (b) a high-quality TH measurement.

Appendix B. Appendix

Table B1
Overview of the allometric equations used for error propagation of DBH (diameter at breast height) and TH (tree height) measurement errors into the total aboveground biomass (AGB). The DBH and TH values are the medians for trees in this study. P is the wood density taken from GWDD v2.2. The AGB error is propagated from the TQ high-quality data measurement errors (DBH MAE of 6% and TH MAE of 11%). The allometric equation coefficients (a, b, and c) can be found in their reference under the Source column.

Species	Equation	Source	DBH [cm]	TH [m]	P [g/cm^3]	AGB Error [%]
Quercus robur	$ln(AGB\ln(AGB) = a + b \bullet ln(DBH\mathrm{b} \bullet \ln(DBH)$	(Zianis et al., 2005)	139.3	24.8	0.66	5.77
Fagus sylvatica	$ln(AGB\ln(AGB) = a + b \bullet ln(DBH\mathrm{b} \bullet \ln(DBH) + c \bullet ln(TH\mathrm{c} \bullet \ln(TH)$	(Zianis et al., 2005)	54.2	12.7	0.56	15.52
Pinus nigra	$AGB = a + b \bullet TH \bullet DBH^2 + c \bullet DBH^2 a + \mathrm{b} \bullet \mathrm{TH} \bullet \mathrm{DBH}^2 + \mathrm{c} \bullet \mathrm{DBH}^2$	(Muukkonen and Mäkipää, 2006)	75.45	20.4	0.41	12.48
Quercus robur	$AGB = a \bullet (\rho \bullet TH \bullet DBH^2)^b a \bullet (\rho \bullet TH \bullet \mathrm{DBH}^2)^b$	(Chave et al., 2014)	139.3	24.8	0.66	9.08
Fagus sylvatica	$AGB = a \bullet (\rho \bullet TH \bullet DBH^2)^b a \bullet (\rho \bullet TH \bullet \mathrm{DBH}^2)^b$	(Chave et al., 2014)	54.2	12.7	0.56	19.8
Pinus nigra	$AGB = a \bullet (\rho \bullet TH \bullet DBH^2)^b a \bullet (\rho \bullet TH \bullet \mathrm{DBH}^2)^b$	(Chave et al., 2014)	75.45	20.4	0.41	13.25

Data availability

I have shared the links to my code and data in the manuscript under the Data and Code Availability section

References

Ahamed, A., Foye, J., Poudel, S., Trieschman, E., Fike, J., 2023. Measuring tree diameter with photogrammetry using mobile phone cameras. Forests 14 (10), 1–16.

Amos, H.M., Starke, M.J., Rogerson, T.M., Colón Robles, M., Andersen, T., Boger, R., Campbell, B.A., Low, R.D., Nelson, P., Overoye, D., Taylor, J.E., Weaver, K.L., Ferrell, T.M., Kohl, H., Schwerin, T.G., 2020. GLOBE observer data: 2016–2019. Earth Space Sci. 7, e2020EA001175.

Araza, A., de Bruin, S., Herold, M., Quegan, S., Labriere, N., Rodriguez-Veiga, P., Avitabile, V., Santoro, M., Mitchard, E.T.A., Ryan, C.M., Phillips, O.L., Willcock, S., Verbeeck, H., Carreiras, J., Hein, L., Schelhaas, M.-J., Pacheco-Pascagaza, A.M., da Conceição Bispo, P., Laurin, G.V., Vieilledent, G., Slik, F., Wijaya, A., Lewis, S.L., Morel, A., Liang, J., Sukhdeo, H., Schepaschenko, D., Cavlovic, J., Gilani, H., Lucas, R., 2022. A comprehensive framework for assessing the accuracy and uncertainty of global above-ground biomass maps. Remote Sens. Environ. 272, 112917.

Azavea, Urban Ecos, 2025. OpenTreeMap. GitHub. https://opentreemap.github.io/ (Accessed: 27.12.2025).

Banda, F., Giorgi, E., Piantanida, R., D'Aria, D., & Mazzucchelli, P. (2025a). BIOMASS Forest Height Products Format Specification. In (p. 68). ESA - ESRIN: ESA.

Banda, F., Giorgi, E., Riccardo, P., D'Aria, D., & Mazzucchelli, P. (2025b). BIOMASS Above Ground Biomass Products Format Specification. In (p. 80). ESA - ESRIN: ESA.

Bobrowski, R., Winczek, M., Zięba-Kulawik, K., Wężyk, P., 2023. Best practices to use the iPad pro LiDAR for some procedures of data acquisition in the urban forest. Urban For. Urban Green. 79, 127815.

Bonnet, P., Joly, A., Faton, J.-M., Brown, S., Kimiti, D., Deneu, B., Servajean, M., Affouard, A., Lombardo, J.-C., Mary, L., Vignau, C., Munoz, F., 2020. How citizen scientists contribute to monitor protected areas thanks to automatic plant identification tools. Ecol. Solut. Evid. 1, e12023.

Bonnet, P., Affouard, A., Chouet, M., Lombardo, J.-C., Gresse, H., Paillot, T., Hequet, V., Goëau, H., Joly, A., 2025. Challenges in using AI-based citizen-generated plant observations as forensic evidence in biodiversity investigations. Biodivers. Inform. Sci. Stand. 9, e181619.

Brede, B., Lau, A., Bartholomeus, H.M., Kooistra, L., 2017. Comparing RIEGL RiCOPTER UAV LiDAR derived canopy height and DBH with terrestrial LiDAR. Sensors 17 (10), 2371.

Buerli, M., Misslinger, S., 2017. Introducing ARKit: Augmented reality for iOS. In: Apple Worldwide Developers Conference (WWDC'17). Apple Inc, San Jose, California.

Çakir, G.Y., Post, C.J., Mikhailova, E.A., Schlautman, M.A., 2021. 3D LiDAR scanning of urban forest structure using a consumer tablet. Urban Sci. 5 (4), 88.

Campbell, B.A., 2021. ICESat-2 and the trees around the GLOBE student research campaign: looking at earth's tree height, one tree at a time. Acta Astronaut. 182, 203–207.

Chambers, P., Laato, S., Yoshida, H., Yrttimaa, T., Liimatainen, K., Uhlgren, V.-V., Hamari, J., Hujala, T., Vastaranta, M., Nummenmaa, T., 2025. Gamified augmented reality for data collection in urban forests. Urban For. Urban Green. 113, 129036.

Chave, J., Réjou-Méchain, M., Búrquez, A., Chidumayo, E., Colgan, M.S., Delitti, W.B.C., Duque, A., Eid, T., Fearnside, P.M., Goodman, R.C., Henry, M., Martínez-Yrízar, A., Mugasha, W.A., Muller-Landau, H.C., Mencuccini, M., Nelson, B.W., Ngomanda, A., Nogueira, E.M., Ortiz-Malavassi, E., Pélissier, R., Ploton, P., Ryan, C.M., Saldarriaga, J.G., Vieilledent, G., 2014. Improved allometric models to estimate the aboveground biomass of tropical trees. Glob. Chang. Biol. 20, 3177–3190.

Crocker, E., Condon, B., Almsaeed, A., Jarret, B., Nelson, C.D., Abbott, A.G., Main, D., Staton, M., 2020. TreeSnap: A citizen science app connecting tree enthusiasts and forest scientists. PLANTS, PEOPLE, PLANET 2, 47–52.

Danylo, O., Moorthy, I., Sturn, T., See, L., Laso Bayas, J.C., Domian, D., Fraisl, D., Giovando, C., Girardot, B., Kapur, R., Matthieu, P.P., Fritz, S., 2018. The picture pile tool for rapid image assessment: a demonstration using Hurricane Matthew. ISPRS Ann. Photogramm. Remote Sens. Spatial Inf. Sci. IV-4, 27–32.

Di Cecco, G.J., Barve, V., Belitz, M.W., Stucky, B.J., Guralnick, R.P., Hurlbert, A.H., 2021. Observing the observers: how participants contribute data to iNaturalist and implications for biodiversity science. BioScience 71, 1179–1188.

Duncanson, L., Kellner, J.R., Armston, J., Dubayah, R., Minor, D.M., Hancock, S., Healey, S.P., Patterson, P.L., Saarela, S., Marselis, S., Silva, C.E., Bruening, J., Goetz, S.J., Tang, H., Hofton, M., Blair, B., Luthcke, S., Fatoyinbo, L., Abernethy, K., Alonso, A., Andersen, H.-E., Aplin, P., Baker, T.R., Barbier, N., Bastin, J.F., Biber, P., Boeckx, P., Bogaert, J., Boschetti, L., Boucher, P.B., Boyd, D.S., Burslem, D.F.R.P., Calvo-Rodriguez, S., Chave, J., Chazdon, R.L., Clark, D.B., Clark, D.A., Cohen, W.B., Coomes, D.A., Corona, P., Cushman, K.C., Cutler, M.E.J., Dalling, J.W., Dalponte, M., Dash, J., de-Miguel, S., Deng, S., Ellis, P.W., Erasmus, B., Fekety, P.A., Fernandez-Landa, A., Ferraz, A., Fischer, R., Fisher, A.G., García-Abril, A., Gobakken, T., Hacker, J.M., Heurich, M., Hill, R.A., Hopkinson, C., Huang, H., Hubbell, S.P., Hudak, A.T., Huth, A., Imbach, B., Jeffery, K.J., Katoh, M., Kearsley, E., Kenfack, D., Kljun, N., Knapp, N., Král, K., Krůček, M., Labrière, N., Lewis, S.L., Longo, M., Lucas, R.M., Main, R., Manzanera, J.A., Martínez, R.V., Mathieu, R., Memiaghe, H., Meyer, V., Mendoza, A.M., Monerris, A., Montesano, P., Morsdorf, F., Næsset, E., Naidoo, L., Nilus, R., O'Brien, M., Orwig, D.A., Papathanassiou, K., Parker, G., Philipson, C., Phillips, O.L., Pisek, J., Poulsen, J.R., Pretzsch, H., Rüdiger, C., Saatchi, S., Sanchez-Azofeifa, A., Sanchez-Lopez, N., Scholes, R., Silva, C.A., Simard, M., Skidmore, A., Stereńczak, K., Tanase, M., Torresan, C., Valbuena, R., Verbeeck, H., Vrska, T., Wessels, K., White, J.C., White, L.J.T., Zahabu, E., Zgraggen, C., 2022. Aboveground biomass density models for NASA's global ecosystem dynamics investigation (GEDI) lidar mission. Remote Sens. Environ. 270, 112845.

Enríquez-de-Salamanca, Á., 2025. Botanical databases in EIA: opportunities and challenges. Impact Assess. Proj. Apprais. 43, 302–312.

Enterkine, J., Campbell, B.A., Kohl, H., Glenn, N.F., Weaver, K., Overoye, D., Danke, D., 2022. The potential of citizen science data to complement satellite and airborne lidar tree height measurements: lessons from the GLOBE program. Environ. Res. Lett. 17, 075003.

Feng, Z., Xie, M., Holcomb, A., Keshav, S., 2024. An app for tree trunk diameter estimation from coarse optical depth maps. Eco. Inform. 82, 102774.

Ferster, C.J., Coops, N.C., 2016. Integrating volunteered smartphone data with multispectral remote sensing to estimate forest fuels. Int. J. Digit. Earth 9, 171–196.

Forsman, M., Börlin, N., Holmgren, J., 2016. Estimation of tree stem attributes using terrestrial photogrammetry with a camera rig. Forests 7 (3), 61.

Fraisl, D., See, L., Sturn, T., MacFeely, S., Bowser, A., Campbell, J., Moorthy, I., Danylo, O., McCallum, I., Fritz, S., 2022. Demonstrating the potential of Picture pile as a citizen science tool for SDG monitoring. Environ. Sci. Pol. 128, 81–93.

Friedlingstein, P., O'Sullivan, M., Jones, M.W., Andrew, R.M., Bakker, D.C.E., Hauck, J., Landschützer, P., Le Quéré, C., Luijkx, I.T., Peters, G.P., Peters, W., Pongratz, J., Schwingshackl, C., Sitch, S., Canadell, J.G., Ciais, P., Jackson, R.B., Alin, S.R., Anthoni, P., Barbero, L., Bates, N.R., Becker, M., Bellouin, N., Decharme, B., Bopp, L., Brasika, I.B.M., Cadule, P., Chamberlain, M.A., Chandra, N., Chau, T.T.T., Chevallier, F., Chini, L.P., Cronin, M., Dou, X., Enyo, K., Evans, W., Falk, S., Feely, R. A., Feng, L., Ford, D.J., Gasser, T., Ghattas, J., Gkritzalis, T., Grassi, G., Gregor, L., Gruber, N., Gürses, Ö., Harris, I., Hefner, M., Heinke, J., Houghton, R.A., Hurtt, G.C., Iida, Y., Ilyina, T., Jacobson, A.R., Jain, A., Jarníková, T., Jersild, A., Jiang, F., Jin, Z., Joos, F., Kato, E., Keeling, R.F., Kennedy, D., Klein Goldewijk, K., Knauer, J., Korsbakken, J.I., Körtzinger, A., Lan, X., Lefèvre, N., Li, H., Liu, J., Liu, Z., Ma, L., Marland, G., Mayot, N., McGuire, P.C., McKinley, G.A., Meyer, G., Morgan, E.J., Munro, D.R., Nakaoka, S.I., Niwa, Y., O'Brien, K.M., Olsen, A., Omar, A.M., Ono, T.,

Paulsen, M., Pierrot, D., Pocock, K., Poulter, B., Powis, C.M., Rehder, G., Resplandy, L., Robertson, E., Rödenbeck, C., Rosan, T.M., Schwinger, J., Séférian, R., Smallman, T.L., Smith, S.M., Sospedra-Alfonso, R., Sun, Q., Sutton, A.J., Sweeney, C., Takao, S., Tans, P.P., Tian, H., Tilbrook, B., Tsujino, H., Tubiello, F., van der Werf, G. R., van Ooijen, E., Wanninkhof, R., Watanabe, M., Wimart-Rousseau, C., Yang, D., Yang, X., Yuan, W., Yue, X., Zaehle, S., Zeng, J., Zheng, B., 2023. Global Carbon Budget 2023. Earth Syst. Sci. Data 15, 5301–5369.

Google, . ARCore Supported Devices. *https://developers.google.com/ar/devices*. Google for Developers: Google.

Grube-Forst GmbH. Durchmesser-Stahlbandmaß. In. https://www.grube.at/p/durchmesser-stahlbandmass/P84-633/?q=massband#itemId=84-635: Grube-Forst GmbH.

Hart, A.G., Bosley, H., Hooper, C., Perry, J., Sellors-Moore, J., Moore, O., Goodenough, A.E., 2023. Assessing the accuracy of free automated plant identification applications. People Nat. 5, 929–937.

Holvoet, J., Eichhorn, M.P., Giannetti, F., Kükenbrink, D., Liang, X., Mokroš, M., Novotný, J., Pitkänen, T.P., Puliti, S., Skudnik, M., Stereńczak, K., Terryn, L., Vega, C., Torresan, C., 2025. Terrestrial and mobile laser scanning for national forest inventories: from theory to implementation. Remote Sens. Environ. 329, 114947.

Hyyppä, J., Virtanen, J.-P., Jaakkola, A., Yu, X., Hyyppä, H., Liang, X., 2018. Feasibility of Google Tango and Kinect for crowdsourcing forestry information. Forests 9 (1), 6.

Iglhaut, J., Cabo, C., Puliti, S., Piermattei, L., O'Connor, J., Rosette, J., 2019. Structure from motion photogrammetry in forestry: a review. Curr. For. Rep. 5, 155–168.

Kangas, A., Astrup, R., Breidenbach, J., Fridman, J., Gobakken, T., Korhonen, K.T., Maltamo, M., Nilsson, M., Nord-Larsen, T., Næsset, E., Olsson, H., 2018. Remote sensing and forest inventories in Nordic countries – roadmap for the future. Scand. J. For. Res. 33, 397–412.

Kükenbrink, D., Marty, M., Rehush, N., Abegg, M., Ginzler, C., 2025. Evaluating the potential of handheld mobile laser scanning for an operational inclusion in a national forest inventory – A Swiss case study. Remote Sens. Environ. 321, 114685.

Laino, D., Cabo, C., Prendes, C., Janvier, R., Ordonez, C., Nikonovas, T., Doerr, S., Santin, C., 2024. 3DFin: a software for automated 3D forest inventories from terrestrial point clouds. Forestry 97, 479–496.

Lanham, M., 2018. Learn ARCore - Fundamentals of Google ARCore: Learn to Build Augmented Reality Apps for Android, Unity, and the Web with Google ARCore 1.0. Packt Publishing.

Larjavaara, M., Muller-Landau, H.C., 2013. Measuring tree height: a quantitative comparison of two common field methods in a moist tropical forest. Methods Ecol. Evol. 4, 793–801.

Lau, A., Bentley, L.P., Martius, C., Shenkin, A., Bartholomeus, H., Raumonen, P., Malhi, Y., Jackson, T., Herold, M., 2018. Quantifying branch architecture of tropical trees using terrestrial LiDAR and 3D modelling. Trees 32, 1219–1231.

Lefort, T., Affouard, A., Charlier, B., Lombardo, J.-C., Chouet, M., Goëau, H., Salmon, J., Bonnet, P., Joly, A., 2026. Cooperative learning of Pl@ntNet's artificial intelligence algorithm: how does it work and how can we improve it? Methods Ecol. Evol. 17, 392–403.

Li, X., Chen, W.Y., Sanesi, G., Lafortezza, R., 2019. Remote sensing in urban forestry: recent applications and future directions. Remote Sens. 1144.

Liang, X., Kankare, V., Yu, X., Hyyppä, J., Holopainen, M., 2014. Automated stem curve measurement using terrestrial laser scanning. IEEE Trans. Geosci. Remote Sens. 52, 1739–1748.

Liang, X., Kankare, V., Hyyppä, J., Wang, Y., Kukko, A., Haggrén, H., Yu, X., Kaartinen, H., Jaakkola, A., Guan, F., Holopainen, M., Vastaranta, M., 2016. Terrestrial laser scanning in forest inventories. ISPRS J. Photogramm. Remote Sens. 115, 63–77.

Liang, X., Hyyppä, J., Kaartinen, H., Lehtomäki, M., Pyörälä, J., Pfeifer, N., Holopainen, M., Brolly, G., Francesco, P., Hackenberg, J., Huang, H., Jo, H.-W., Katoh, M., Liu, L., Mokroš, M., Morel, J., Olofsson, K., Poveda-Lopez, J., Trochta, J., Wang, D., Wang, J., Xi, Z., Yang, B., Zheng, G., Kankare, V., Luoma, V., Yu, X., Chen, L., Vastaranta, M., Saarinen, N., Wang, Y., 2018. International benchmarking of terrestrial laser scanning approaches for forest inventories. ISPRS J. Photogramm. Remote Sens. 144, 137–179.

Liang, X., Wang, Y., Pyörälä, J., Lehtomäki, M., Yu, X., Kaartinen, H., Kukko, A., Honkavaara, E., Issaoui, A.E.I., Nevalainen, O., Vaaja, M., Virtanen, J.-P., Katoh, M., Deng, S., 2019. Forest in situ observations using unmanned aerial vehicle as an alternative of terrestrial measurements. For. Ecosyst. 6, 20.

Liu, J., Feng, Z., Yang, L., Mannan, A., Khan, T.U., Zhao, Z., Cheng, Z., 2018. Extraction of sample plot parameters from 3D point cloud reconstruction based on combined RTK and CCD continuous photography. Remote Sens. 10 (8), 1299.

Liu, S., Brandt, M., Nord-Larsen, T., Chave, J., Reiner, F., Lang, N., Tong, X., Ciais, P., Igel, C., Pascual, A., Guerra-Hernandez, J., Li, S., Mugabowindekwe, M., Saatchi, S., Yue, Y., Chen, Z., Fensholt, R., 2023. The overlooked contribution of trees outside forests to tree cover and woody biomass across Europe. Sci. Adv. 9, eadh4097.

Luetzenburg, G., Kroon, A., Bjørk, A.A., 2021. Evaluation of the apple iPhone 12 pro LiDAR for an application in geosciences. Sci. Rep. 11, 22221.

Lumnitz, S., Devisscher, T., Mayaud, J.R., Radic, V., Coops, N.C., Griess, V.C., 2021. Mapping trees along urban street networks with deep learning and street-level imagery. ISPRS J. Photogramm. Remote Sens. 175, 144–157.

Luoma, V., Saarinen, N., Wulder, M.A., White, J.C., Vastaranta, M., Holopainen, M., Hyyppä, J., 2017. Assessing precision in conventional field measurements of individual tree attributes. Forests 38.

Magnuson, R., Erfanifard, Y., Kulicki, M., Gasica, T.A., Tangwa, E., Mielcarek, M., Stereńczak, K., 2024. Mobile devices in forest mensuration: a review of technologies and methods in single tree measurements. Remote Sens. 16 (19), 3570.

Magnussen, S., Nord-Larsen, T., Riis-Nielsen, T., 2018. Lidar supported estimators of wood volume and aboveground biomass from the Danish national forest inventory (2012–2016). Remote Sens. Environ. 211, 146–153.

Matney, L., . Google Kills Its Tango Augmented Reality Platform, Shifting Focus to ARCore. https://techcrunch.com/2017/12/15/google-kills-its-tango-augmented-reality-platform-shifting-focus-to-arcore/:. TechCrunch.

McRoberts, R.E., Tomppo, E.O., Næsset, E., 2010. Advances and emerging issues in national forest inventories. Scand. J. For. Res. 25, 368–381.

Mokroš, M., Liang, X., Surový, P., Valent, P., Čerňava, J., Chudý, F., Tunák, D., Saloň, Š., Merganič, J., 2018. Evaluation of close-range photogrammetry image collection methods for estimating tree diameters. ISPRS Int. J. Geo Inf. 7 (3), 93.

Mulverhill, C., Coops, N.C., Tompalski, P., Bater, C.W., Dick, A.R., 2019. The utility of terrestrial photogrammetry for assessment of tree volume and taper in boreal mixedwood forests. Ann. For. Sci. 76, 83.

Muukkonen, P., Mäkipää, R., 2006. Biomass equations for European trees: addendum. Silva Fennica 40, 763–773.

Neuenschwander, A., Duncanson, L., Montesano, P., Minor, D., Guenther, E., Hancock, S., Wulder, M.A., White, J.C., Purslow, M., Thomas, N., Mandel, A., Feng, T., Armston, J., Kellner, J.R., Andersen, H.E., Boschetti, L., Fekety, P., Hudak, A., Pisek, J., Sánchez-López, N., Stereńczak, K., 2024. Towards global spaceborne lidar biomass: developing and applying boreal forest biomass models for ICESat-2 laser altimetry data. Sci. Remote Sens. 10, 100150.

Nowacki, P., Woda, M., 2020. Capabilities of ARCore and ARKit platforms for AR/VR applications. In: Zamojski, W., Mazurkiewicz, J., Sugier, J., Walkowiak, T., Kacprzyk, J. (Eds.), Engineering in Dependability of Computer Systems and Networks. Springer International Publishing, Cham, pp. 358–370.

Nowak, D.J., 2024. Understanding I-Tree: 2023 Summary of Programs and Methods. U.S. Department of Agriculture, Forest Service, Northern Research Station.

Pace, R., Masini, E., Giuliarelli, D., Biagiola, L., Tomao, A., Guidolotti, G., Agrimi, M., Portoghesi, L., De Angelis, P., Calfapietra, C., 2022. Tree measurements in the urban environment: insights from traditional and digital field instruments to smartphone applications. Arboric. Urban For. 48, 113.

Pan, Y., Birdsey, R.A., Phillips, O.L., Houghton, R.A., Fang, J., Kauppi, P.E., Keith, H., Kurz, W.A., Ito, A., Lewis, S.L., Nabuurs, G.-J., Shvidenko, A., Hashimoto, S., Lerink, B., Schepaschenko, D., Castanho, A., Murdiyarso, D., 2024. The enduring world forest carbon sink. Nature 631, 563–569.

Pantera, A., Burgess, P.J., Mosquera Losada, R., Moreno, G., López-Díaz, M.L., Corroyer, N., McAdam, J., Rosati, A., Papadopoulos, A.M., Graves, A., Rigueiro Rodríguez, A., Ferreiro-Domínguez, N., Fernández Lorenzo, J.L., González-Hernández, M.P., Papanastasis, V.P., Mantzanas, K., Van Lerberghe, P., Malignier, N., 2018. Agroforestry for high value tree systems in Europe. Agrofor. Syst. 92, 945–959.

Pascual, A., 2021. Multi-objective forest planning at tree-level combining mixed integer programming and airborne laser scanning. For. Ecol. Manag. 483, 118714.

Pascual, A., Tupinambá-Simões, F., de Conto, T., 2022. Using multi-temporal tree inventory data in eucalypt forestry to benchmark global high-resolution canopy height models. A showcase in Mato Grosso, Brazil. Eco. Inform. 70, 101748.

Pereira, I.S., Mendonça do Nascimento, H.E., Boni Vicari, M., Disney, M., DeLucia, E.H., Domingues, T., Kruijt, B., Lapola, D., Meir, P., Norby, R.J., Ometto, J.P.H.B., Quesada, C.A., Rammig, A., Hofhansl, F., 2019. Performance of laser-based electronic devices for structural analysis of Amazonian terra-firme forests. Remote Sens. 11 (5), 510.

Persson, H.J., Olofsson, K., Holmgren, J., 2022. Two-phase forest inventory using very-high-resolution laser scanning. Remote Sens. Environ. 271, 112909.

Philippsen, M., Mutschler, C., Löffler, C., Steiner, S., Porada, A., Feigl, T., 2020. Localization limitations of ARCore, ARKit, and Hololens in dynamic large-scale industry environments. In: Proceedings of the 15th International Joint Conference on Computer Vision, Imaging and Computer Graphics Theory and Applications, pp. 307–318.

Piermattei, L., Karel, W., Wang, D., Wieser, M., Mokroš, M., Surový, P., Koreň, M., Tomaštík, J., Pfeifer, N., Hollaus, M., 2019. Terrestrial structure from motion photogrammetry for deriving forest inventory data. Remote Sens. 11 (8), 950.

Pl@ntNet, . My Pl@ntNet API - API Service for Developers v2.2.1, OAS2.0. https://my-api.plantnet.org. Pl@ntNet.

Popp, M.R., Zimmermann, N.E., Brun, P., 2025. Evaluating the use of automated plant identification tools in biodiversity monitoring—a case study in Switzerland. Eco. Inform. 90, 103316.

Raumonen, P., Kaasalainen, M., Åkerblom, M., Kaasalainen, S., Kaartinen, H., Vastaranta, M., Holopainen, M., Disney, M., Lewis, P., 2013. Fast automatic precision tree models from terrestrial laser scanner data. Remote Sens. 491–520.

Renner, S.S., 2026. Linking to images and AI-based identification tools—the only way for Flora projects to survive. PLANTS, PEOPLE, PLANET 8, 452–460.

Roman, L.A., Scharenbroch, B.C., Östberg, J.P.A., Mueller, L.S., Henning, J.G., Koeser, A. K., Sanders, J.R., Betz, D.R., Jordan, R.C., 2017. Data quality in citizen science urban tree inventories. Urban For. Urban Green. 22, 124–135.

Roy, S., Byrne, J., Pickering, C., 2012. A systematic quantitative review of urban tree benefits, costs, and assessment methods across cities in different climatic zones. Urban For. Urban Green. 11, 351–363.

Saarela, S., Grafström, A., Ståhl, G., Kangas, A., Holopainen, M., Tuominen, S., Nordkvist, K., Hyyppä, J., 2015. Model-assisted estimation of growing stock volume using different combinations of LiDAR and Landsat data as auxiliary information. Remote Sens. Environ. 158, 431–440.

Saarinen, N., Vastaranta, M., Kankare, V., Tanhuanpää, T., Holopainen, M., Hyyppä, J., Hyyppä, H., 2014. Urban-tree-attribute update using multisource single-tree inventory. Forests 1032–1052.

Santoro, M., Cartus, O., Carvalhais, N., Rozendaal, D.M.A., Avitabile, V., Araza, A., de Bruin, S., Herold, M., Quegan, S., Rodríguez-Veiga, P., Balzter, H., Carreiras, J., Schepaschenko, D., Korets, M., Shimada, M., Itoh, T., Moreno Martínez, Á., Cavlovic, J., Cazzolla Gatti, R., da Conceição Bispo, P., Dewnath, N., Labrière, N., Liang, J., Lindsell, J., Mitchard, E.T.A., Morel, A., Pacheco Pascagaza, A.M., Ryan, C. M., Slik, F., Vaglio Laurin, G., Verbeeck, H., Wijaya, A., Willcock, S., 2021. The global forest above-ground biomass pool for 2010 estimated from high-resolution satellite observations. Earth Syst. Sci. Data 13, 3927–3950.

Schadauer, K., Astrup, R., Breidenbach, J., Fridman, J., Gräber, S., Köhl, M., Korhonen, K.T., Johannsen, V.K., Morneau, F., Päivinen, R., Riedel, T., 2024. Access to exact National Forest Inventory plot locations must be carefully evaluated. New Phytol. 242, 347–350.

Schmidt, R.J., Casario, B.M., Zipse, P.C., Grabosky, J.C., 2022. An analysis of the accuracy of photo-based plant identification applications on fifty-five tree species. Arboric. Urban For. 27–43.

Schnell, S., Altrell, D., Ståhl, G., Kleinn, C., 2014. The contribution of trees outside forests to national tree biomass and carbon stocks—a comparative study across three continents. Environ. Monit. Assess. 187, 4197.

Seabold, S., Perktold, J., 2010. Statsmodels: econometric and statistical modeling with python. In: 9th Python in Science Conference.

See, L., Comber, A., Salk, C., Fritz, S., van der Velde, M., Perger, C., Schill, C., McCallum, I., Kraxner, F., Obersteiner, M., 2013. Comparing the quality of crowdsourced data contributed by expert and non-experts. PLoS One 8, e69958.

Smith, M.M., Bentrup, G., Kellerman, T., MacFarland, K., Straight, R., Ameyaw, L., 2021. Windbreaks in the United States: A systematic review of producer-reported benefits, challenges, management activities and drivers of adoption. Agric. Syst. 187, 103032.

Smithers, R.J., Doick, K.J., Burton, A., Sibille, R., Steinbach, D., Harris, R., Groves, L., Blicharska, M., 2018. Comparing the relative abilities of tree species to cool the urban environment. Urban Ecosyst. 21, 851–862.

Tomaštík Jr., J., Tomaštík Sr., J., Saloň, Š., Piroh, R., 2017. Horizontal accuracy and applicability of smartphone GNSS positioning in forests. Forestry 90, 187–198.

van Doorn, N.S., Roman, L.A., McPherson, E.G., Scharenbroch, B.C., Henning, J.G., Östberg, J.P.A., Mueller, L.S., Koeser, A.K., Mills, J.R., Hallet, R.A., Sanders, J.E., Battles, J., Boyer, D.J., Fristensky, J.P., Mincey, S.K., Peper, P.J., Vogt, J.M., 2020. Urban Tree Monitoring: A Resource Guide. U.S. Department of Agriculture, Forest Service, Pacific Southwest Research Station.

Vauhkonen, J., 2020. Effects of diameter distribution errors on stand management decisions according to a simulated individual tree detection. Ann. For. Sci. 77, 21.

Vosselman, G., Maas, H.-G., 2010. Airborne and Terrestrial Laser Scanning. Whittles Publishing, Dunbeath.

Wang, Y., Bakker, F., de Groot, R., Wortche, H., Leemans, R., 2015. Effects of urban trees on local outdoor microclimate: synthesizing field measurements by numerical modelling. Urban Ecosyst. 18, 1305–1331.

Westfall, J.A., Henning, J.G., Edgar, C.B., 2021. Urban tree measurement variability and the contribution to uncertainty in estimates of ecosystem services. Urban For. Urban Green. 64, 127302.

Wu, F., Wu, B., Zhao, D., 2023. Real-time measurement of individual tree structure parameters based on augmented reality in an urban environment. Eco. Inform. 77, 102207.

Zhao, N., Prieur, J.-F., Liu, Y., Kneeshaw, D., Lapointe, E.M., Paquette, A., Zinszer, K., Dupras, J., Villeneuve, P.J., Rainham, D.G., Lavigne, E., Chen, H., van den Bosch, M., Oiamo, T., Smargiassi, A., 2021. Tree characteristics and environmental noise in complex urban settings – a case study from Montreal, Canada. Environ. Res. 202, 111887.

Zianis, D., Muukkonen, P., Mäkipää, R., Mencuccini, M., 2005. Biomass and stem volume equations of tree species in Europe. Silva Fenn. 4.